VOL. 13 No. 12 pp. 337-372 JUNE 1952

Philips Technical Review

DEALING WITH TECHNICAL PROBLEMS
RELATING TO THE PRODUCTS, PROCESSES AND INVESTIGATIONS OF
THE PHILIPS INDUSTRIES

EDITED BY THE RESEARCH LABORATORY OF N.V. PHILIPS' GLOEILAMPENFABRIEKEN, EINDHOVEN, NETHERLANDS

THERMIONIC EMITTERS UNDER PULSED OPERATION

by R. LOOSJES, H. J. VINK and C. G. J. JANSEN.

537.583: 621.385.032.216

The sphere of electronics has become so extensive that those who are employed in the design of circuits for specific purposes may easily lose sight of the physical principles of the medium in which they work. Although this need not be a deterrent to devising new, and even more ingenious, circuits, it should, nevertheless, be realized that real progress in the sphere of electronics can only be made through painstaking and patient study of the basic principles. These are, in the first place, the physical processes in an electronic tube, and the emission of electrons from the cathode is one of the most important. An investigation of this emission in the special case of pulsed operation — so important for radar — has shown that some very remarkable and entirely unexpected physical phenomena occur, of which the consequences cannot yet be fully grasped.

The use of thermionic emitters in valves for pulsed operation has become of the utmost importance during the last ten years. By pulsed operation is understood causing a cathode to emit intensively for a short period (for example 1-100 μsec) followed by a comparatively long interval (for example 1000 μsec).

The application of pulsed operation is of great importance in radar, apart from many other things. The use of pulses creates, in the first place, the possibility for a clear echo effect. Moreover, it is possible to obtain, with a comparatively small valve, a very large temporary output. This was already discovered in 1940, thus enabling the rapid development of radar. The extent of the difference in behaviour at pulsed and D.C. operation is made clear by the fact that a normal oxide-coated cathode ((BaSr)O) can supply current densities of tens of amps per cm^2 for one microsecond, whereas at D.C. operation the emission cannot be more than a few hundreds of milliamps per cm^2. It is therefore not surprising that this curious behaviour of the oxide-coated cathode should have been studied by a number of investigators ¹).

These investigations were divided mainly into research into two different problems. The more practical one was designed to find the limits of thermionic emission for pulsed operation. The other, more theoretical, problem was designed to investigate what exactly happened in the oxide-coated cathode during a pulse and why there should be such a considerable difference between D.C. and pulsed emission.

Despite most intensive investigations, there is still no conclusive reply to the latter questions. In this article, an idea is given of the investigations which have been conducted in this direction in the Philips Laboratories at Eindhoven and a report of the remarkable phenomena which were found. Particularly remarkable is that the gradient of the potential in the oxide coating differs considerably from that in a normal resistor, and that the velocities of the electrons which are emitted by the oxide-coated cathode are not distributed according to Maxwell's rule (this would mean that the greatest differences in velocities that occur would amount to a few tenths of eV), but that the emitted electrons can be divided into several groups having different velocities. The velocities of the groups appear to differ by from some tens to some hundreds of eV.

---

¹) See, for example, E. A. Coomes, J. appl. Phys. **17**, 646, 1946. M. H. Pomerantz, Proc. I. R. E. **34**, 903, 1946. A. S. Eisenstein, Advances in Electronics **1**, 1, 1948.

Before the apparatus used to measure the velocity spectra is described and before discussing the results obtained in this manner, a short review will be given of the published results of other investigators of the behaviour of thermionic emitters for pulsed operation. This will be followed by a description of our investigations concerning the potential gradient in the oxide coating of the cathode. It were the results of these investigations which led us to investigate the velocity distribution. Finally, we shall sum up the consequences of the spectra found, as applied to the use of cathodes for pulsed operation.

Published results of other investigators

The investigations mentioned in the footnote [1]) resulted in a number of findings of great practical and theoretical importance. It was established, for example, that the maximum pulsed emission that can be obtained from an oxide-coated cathode is just over 100 A/cm^2. Moreover, it was found that with a new cathode this current density and the concomitant anode voltage corresponded to a point on that part of the current-voltage characteristic which is determined by the presence of space charge (see *fig. 1*, point P). The fact that the emission cannot be further increased by increasing the anode voltage is due to the occurrence of sparking. It is easy to understand that this sparking is not a normal breakdown between cathode and anode. When a normal breakdown occurs, the field strength at the surface of the cathode must be large, and positive in the direction of the anode. This is not possible as long as a negative space charge is present near the cathode. All this is true only for cathodes which are comparatively new. With older cathodes the current-voltage characteristic is slightly lower, and the current is saturated at a sufficiently high voltage, causing sparking to occur in the saturation area (see fig. 1, point Q). In that case there is a strong electrical field at the surface of the cathode which draws the electrons from the cathode.

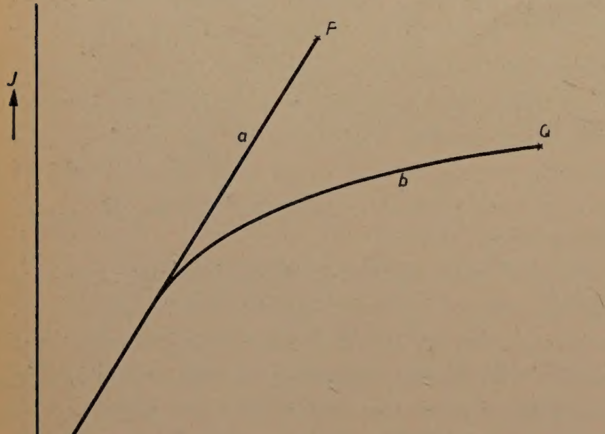

Fig. 1. Current-density-voltage-characteristic of a thermionic emitter under pulsed conditions. A potential gradient is caused by the negative space-charge present in front of the cathode provided the temperature is not too low and the voltage not too high, so that not all the electrons emitted can reach the anode. In that case $J \sim V_a^{3/2}$ (Langmuir-Child formula) is true. When increasing the anode voltage V_a in excess of a certain value, the space charge no longer influences the emission and so-called saturation occurs. In the characteristic, in which J has been plotted against $V_a^{3/2}$, this is shown by a deviation from a straight line. With a new cathode (curve a) sparking occurs in that part of the characteristic determined by the space charge (P); with an old cathode (curve b) sparking occurs in the saturation area (Q).

Another very important property, in addition to the maximum density of the current, is the electrical resistance of the oxide coating. This determines the additional heating of the cathode during the period of emission. At pulsed operation this additional heating (which is proportional to the resistance R and the square of the current density i) may be considerable at average current strengths which would have only a slight heating effect at D.C. operation. An increase in cathode temperature to the extent of 50 °C, as a result of the passage of a pulse current, is not exceptional.

Apart from the normal electrical resistance of the entire oxide coating, there may be also other resistances in the interfacial area between the metal base and the oxide coating. These resistances may be greater than those of the oxide coating itself. resulting in a large potential fall in the interface layer which, in turn, can lead to the greatest part of the heat due to the Joule effect being developed in that layer. It is assumed that the combination of high temperature and great field strength may be the cause of sparking.

The high resistance of the interface layer is caused by coumpounds resulting from reactions between the oxide coating on the one hand and the reducing components (for example Si, Ti), which are present as impurities in the nickel cathode base on the other hand. In other words; this high-resistance layer consists of bariumsilicate, barium titanate and similar substances. As such, reducing reactions are indispensable to obtaining good emission from an oxide-coated cathode, although a high-resistance layer is undesired because it influences sparking, an attempt has been made to reduce the influence of the resistance layer and a search has also been made for reducing materials which will not form such a layer. Our investigations have thrown a little light on the last-mentioned point, i.e. the avoidance of a layer with a high resistance. A description of this will be given later. Some reduction of the influence of the resistance layer is achieved by constructions in which a skeleton of nickel is incorporated in the oxide coating [2]). This reduces the interface resistance as a result of the larger contact surface between nickel and oxide.

A description of our own studies and of the phenomena which we observed, some of which have not hitherto been published, follows. These notes may be valuable in explaining the occurrence of heating in the oxide coating and sparking phenomena.

The potential gradient in the oxide coating

Method of measurement

Two methods were used to investigate the potential gradient in the oxide coating during a current pulse. The first method [3]) was intended to give an overall picture of the total potential drop through the total thickness of the oxide coating. Diodes, with a flat cathode and adjustable anode, were used for this purpose (see *fig. 2*). The voltage between cathode and anode (V_a) is determined at a certain current pulse and the anode is brought closer to the cathode, step by step. The relation found between V_a and the distance between anode and cathode was extrapolated to the zero distance in the assumption that the difference in potential established in this way would be the voltage through the oxide coating [4]).

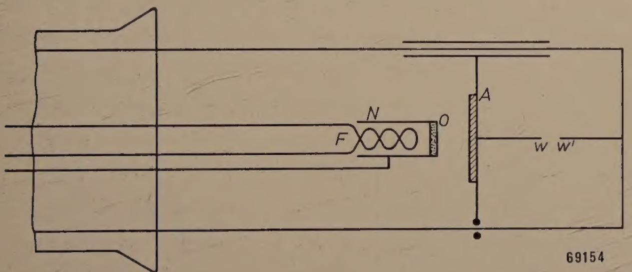

Fig. 2. Diode for measuring the potential gradient across the oxide coating. *F* filament, *N* nickel cathode base, *O* oxide coating, *A* adjustable anode. The distance between anode and cathode is determined by the distance between the points *W* and *W'*.

It would have been simpler and more direct to measure the potential difference whilst the anode was pressed against the cathode. This was indeed done; but when comparing these results with the result obtained by extrapolating to zero distance, it appeared that the two potential differences obtained varied considerably. This led to the conclusion that for pulsed operation the measurements were seriously disturbed by the contact between cathode and anode. This conclusion was supported by the fact that, when the cathode and anode were pressed together, sparking was observed.

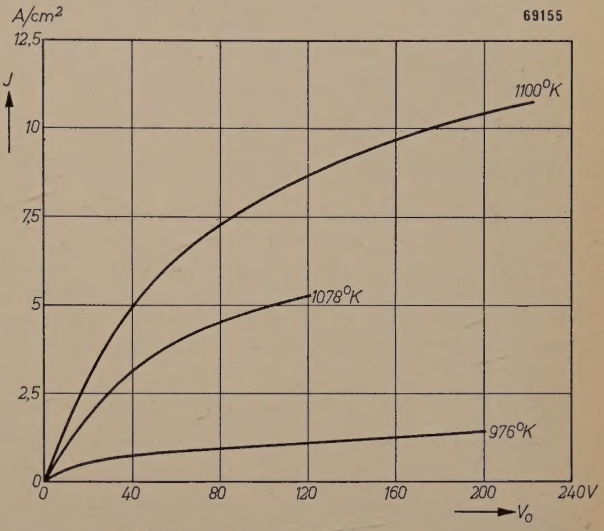

Fig. 3. Current-density-voltage-characteristics of an oxide-coated cathode under pulsed conditions at different temperatures. The voltage V_0 is plotted for the whole of the oxide coating as a function of the current density J. Total thickness of the oxide coating 25 μ.

The J-V characteristics at different temperatures, illustrated in *fig. 3*, were found by measuring, in addition to the potential gradient V through the oxide coating, also the current per cm² (J) emitted by the cathode. The graph shows that very great differences in potential (a few hundreds of volts) may occur in the oxide coating.

The next problem was to investigate the distribution of the potential gradient through the thickness of the coating: whether it was evenly distributed through the total thickness or whether it was localized in a certain part of the coating (for example, in the interface layer between nickel and oxide).

In order to investigate this potential gradient, one or more metal probes were placed in the oxide coating. A drawback of this method is, of course, that, in spite of the fineness of the wires used (thickness 8 μ), these might cause a considerable disturbance in the situation within the layer. We think, however, that the results found in this way, are, nevertheless, broadly correct for the potential gradient in the cathode.

---

[2]) Cathodes of this type are made in the first place to improve the bond between the oxide and the nickel. It was feared that strong electrical fields would pull the oxide away.

[3]) R. Loosjes and H. J. Vink, Philips Res. Rep. 2, 190, 1947.

[4]) The justification, proving the result obtained by means of extrapolation, is given in the article referred to in footnote [3]).

Fig. 4 gives an idea of the potential differences which were found, at different current densities, between the metal base of a cathode and three probes placed at distances of resp. 35 μ, 85 μ and 180 μ from the base. (The tests were made with a cathode covered with an oxide coating having a thickness of 270 μ). The fact that the potential difference between the nickel cathode base and the first probe and that between the second probe and the first were of the same order, was conspicuous. It meant that there was no extraordinarily large potential difference between the metal base and the first probe in this case; this is contrary to the experience of most other investigators.

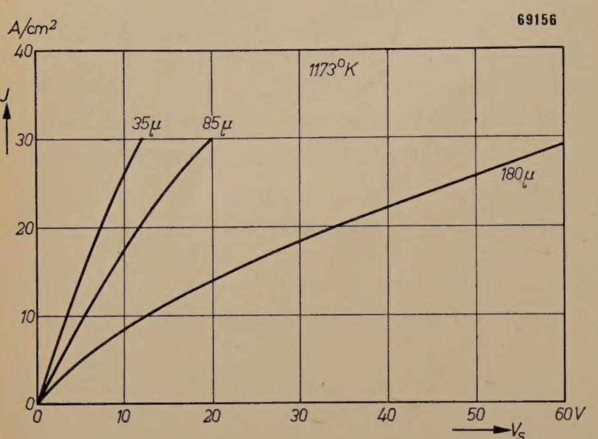

Fig. 4. Potential difference V_s between metal base and probes in the oxide coating as a function of the current density J. As is indicated, the various lines belong to probes which were placed at distances of 35 μ, 85 μ and 180 μ, respectively.

As the total potential difference across the oxide coating is much greater, with a coating of only 25 μ thick, than the above-mentioned potential differences between probes and nickel base (see fig. 3), we can only conclude that the potential gradient found by us for the total layer must be localized mainly somewhere near the surface.

The potential gradient as a function of the distance to the metal base, in a diode during a pulse, must therefore be as sketched in *fig. 5a*. The way in which this potential gradient was generally thought to be, has also been illustrated for purposes of comparison (fig. 5*b*). The absence of an area with large resistance in the boundary layer between metal and oxide is probably to be ascribed to the cathode nickel used by us. The contamination consisted principally of 0.1% to 0.2% magnesium and some silicon. The boundary layers with large resistance were found mostly when nickel had been used which contained principally silicon or chromium. Reverting to a remark made in the introduction, it is now clear that there are kinds of nickel in which there will not be an interfacial layer with large resistance.

This conclusion concerning a layer with large resistance close to the surface was tested by investigating an effect which might be expected from a potential distribution as illustrated in fig. 5*a*. The very porous structure of the oxide coating (50 to 80% pores; see also fig. 11) must lead to the assumption that the electrons are emitted not only from the surface but also from places deeper

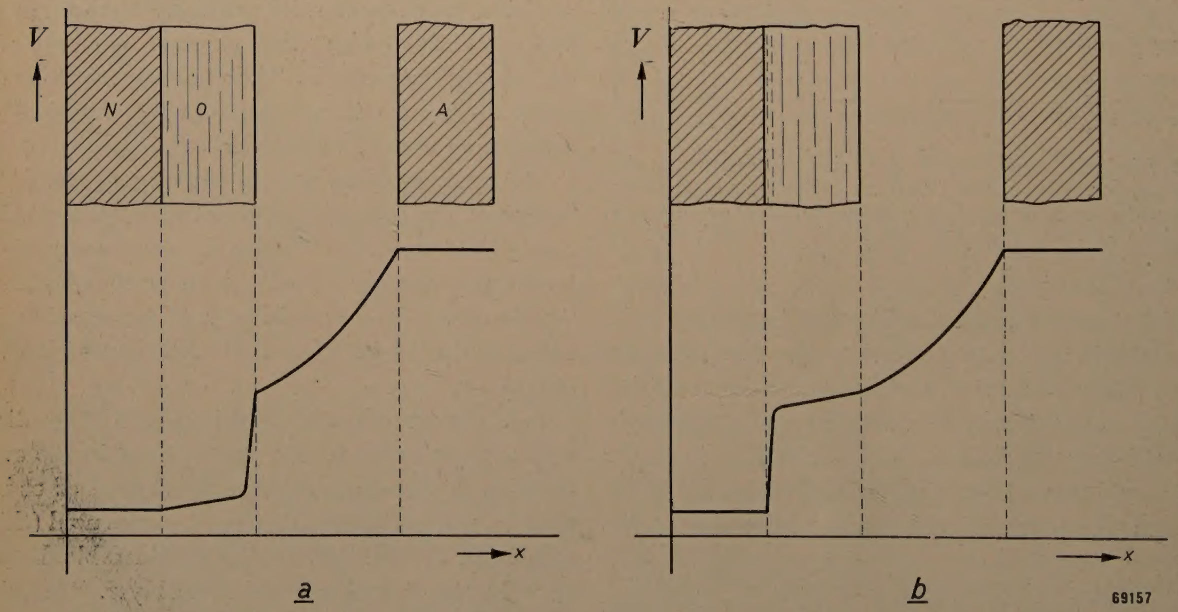

Fig. 5. Potential gradient in a diode during a pulse, according to our measurements (*a*) and according to Eisenstein (*b*) (see the article mentioned in footnote [1])). *N* metal base, *O* oxide coating, *A* anode.

in the coating. As the latter pass through a fairly large potential difference before arriving at the surface, it was to be expected that the emitted electrons would have velocities which differ by some tens of electron volts from each other. The velocity distribution of the electrons must, therefore, deviate from the Maxwell distribution which implies, as we have already remarked, that the differences are only a few tenths of electronvolts at a working temperature of 800 °C. This led us to investigate the velocity distribution of the emitted electrons.

The velocity distribution of emitted electrons

Description of the measuring tube

A special tube was constructed (*fig. 6*) to measure, in the best possible way, the velocity of emitted electrons. The principal parts of this tube were: the cathode (*K*), the anode (*A*) with a round aperture with a diameter of 200 μ, a screen (*B*) with a round aperture with a diameter of 4 mm, and a collector (*C*), with a rectangular slit measuring 24 mm × 0.3 mm. Deflection plates (*D*) were constructed behind the collector and, finally, a fluorescent screen (*Fl*).

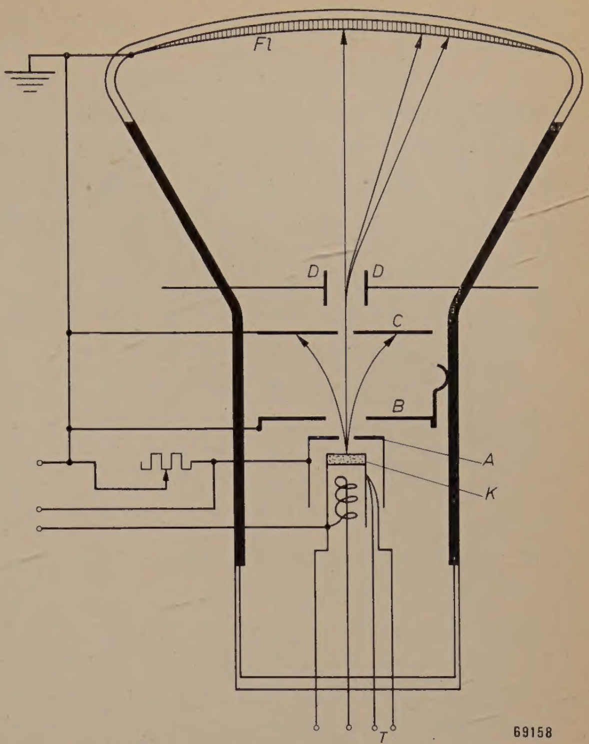

Fig. 6. Tube for determining the velocity distribution of the emitted electrons. *K* cathode, *A* anode, *B* screen, *C* collector, *D* deflection plates, *Fl* fluorescent screen, *T* thermocouple.

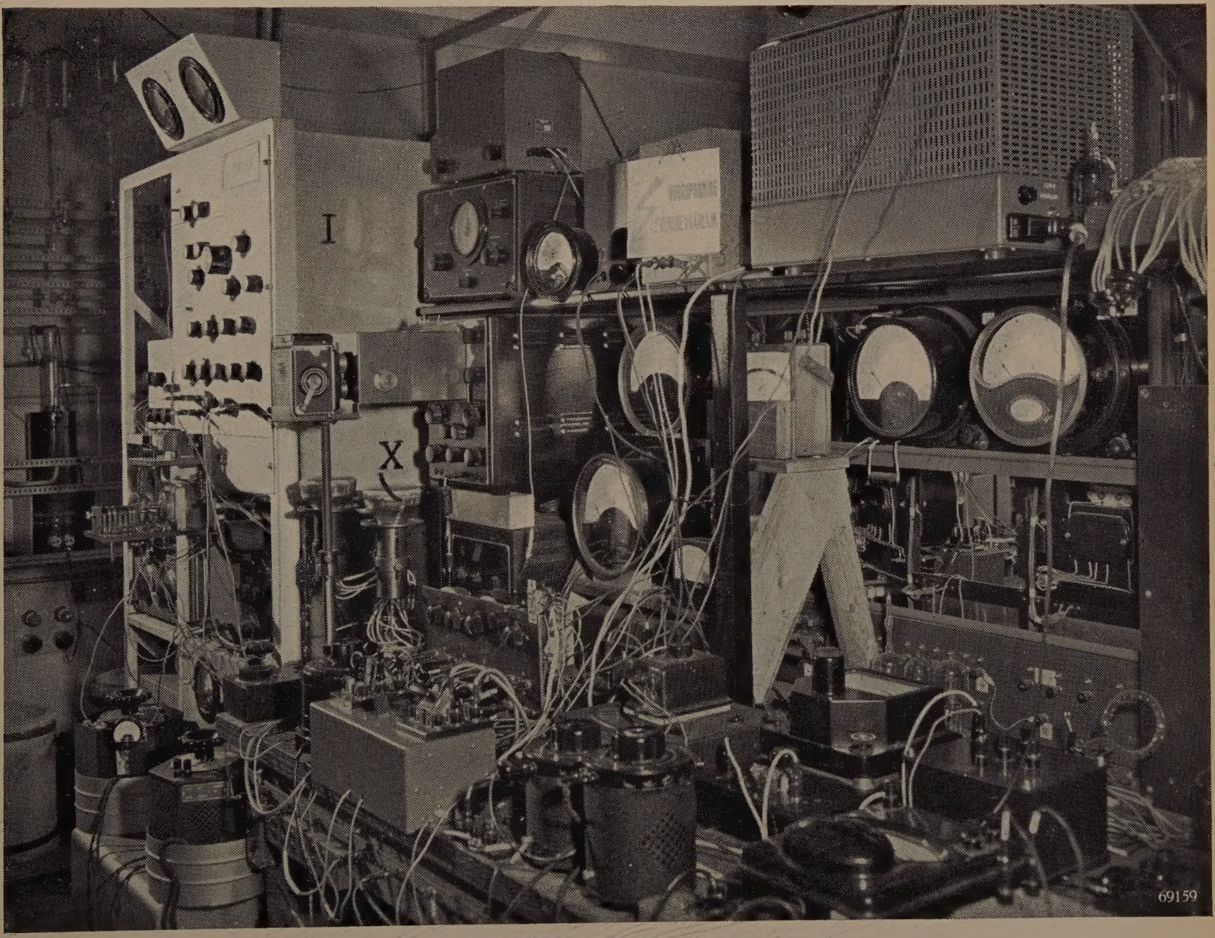

Fig. 7. Set-up for measuring electron velocity spectra. *X* measuring tube. *I* pulse generator.

Fig. 7 gives a general idea of the complete apparatus used for these measurements.

Operation of the measuring tube

If the cathode is at a negative potential with respect to the anode, part of the electrons flowing to the anode will pass through the aperture in the anode and enter the equipotential space behind the anode. The lens effect of the anode diaphragm and electrostatic repulsion between the electrons themselves, will cause the beam to spread. Because of this, only part of the beam will pass through the slit in the collector *C*. If both the deflection plates are at anode potential, the electron beam will form a sharp picture of the slit upon the fluorescent screen. If a potential difference is applied across the deflection plates, the place where an electron strikes the screen *Fl* will depend upon its velocity: the image of the slit will change into a spectrum. From the spectra obtained in this manner it was indeed shown that normal oxide-coated cathodes ((BaSr)O) will emit electrons, during a square-wave pulse, at velocities which, in some cases, varied by as much as two hundred electron volts.

A more detailed description will now be given of the velocity spectra found.

Resultant spectra

A number of characteristic electron velocity spectra are shown in *fig. 8*. Besides investigating the emission from (BaSr)O-cathodes, we also examined the spectra of a number of other kinds of cathodes. It must be admitted that the spectra of different cathodes, although coated with the same oxide (for example (BaSr)O) at a temperature of, for example, 925 °C 5), are not identical with the one illustrated in fig. 8*b*. This spectrum is, however, representative of the behaviour of the majority of different (BaSr)O-cathodes at that temperature.

In the spectra of a tantalum cathode or an L-cathode 6) (both metallic cathodes without an oxide coating) we can observe only one sharp line, thus electrons of one velocity, and the velocity corresponds to that which the electrons possess as a result of the acceleration in the field between the cathode and the anode. This is in accordance with expectations, as we would not be able to observe a Maxwell distribution and these metallic cathodes have no noticeable resistance; this signifies that all electrons are emitted from places having practically the same potential. These spectra also indicate that the tubes we used do not cause "false" lines, for example, due to secondary emission of the anode.

The spectrum of the normal oxide-coated cathode ((BaSr)O) shows the curious phenomenon referred to in the introduction; that there is not only a considerable range of electron velocities (to be expected in view of the potential gradient in the oxide coating), but that there are discrete lines, which mean that the electrons are divided into groups having certain velocities. It may further be observed that the velocity of even the fastest

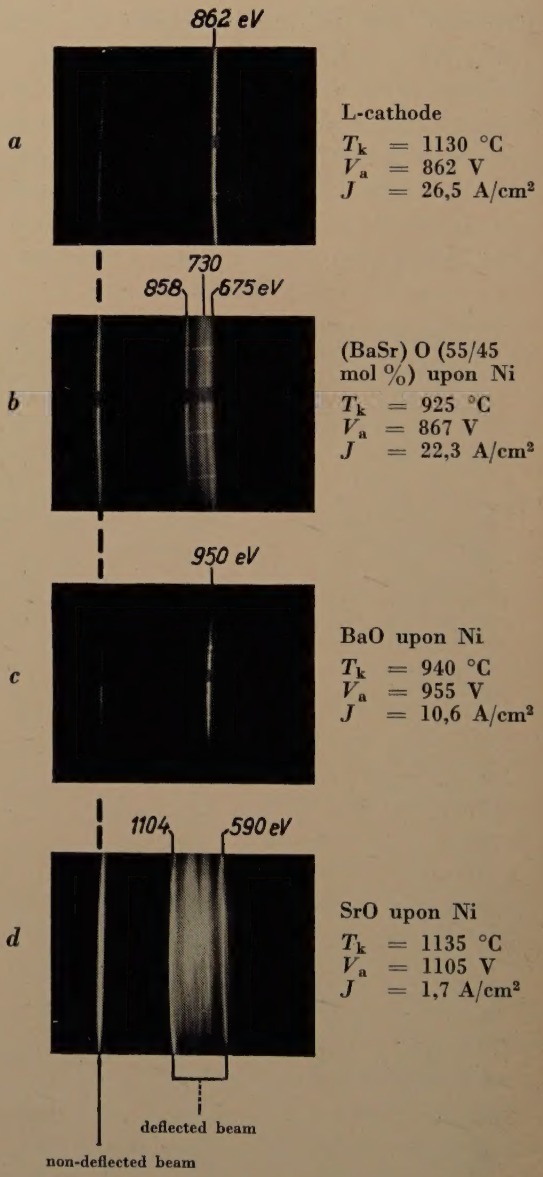

Fig. 8. Electron velocity spectra for different kinds of cathodes under square-pulsed operation. Pulse width ≈ 2.10^{-6} sec. The pulse recurrence frequency in *a*, *b*, *c* and *d* was 1000, 500, 1000 and 6000 c/s, respectively. The thickness of the oxide coating of *b*, *c* and *d* was about 60 μ.

---

5) All the temperatures communicated have been measured by means of thermo couples (see *T* in fig. 6): these are, therefore, so-called true temperatures.

6) See H. J. Lemmens, M. J. Jansen and R. Loosjes, A new thermionic cathode for heavy loads, Philips Techn. Rev. **11**, 341-350, 1949/1950.

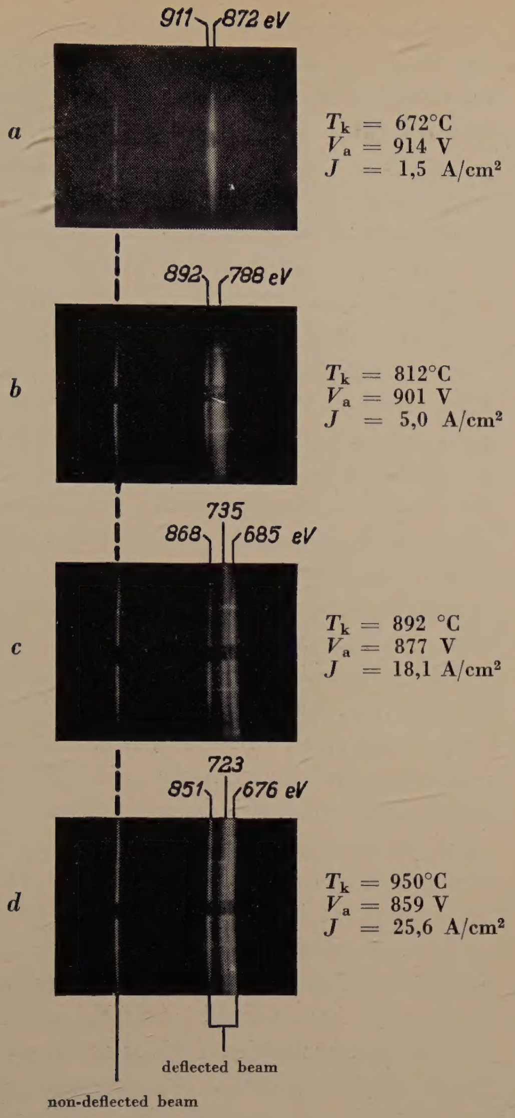

Fig. 9. Electron velocity spectra of a (BaSr)O-cathode (55/45 mol %) at different temperatures; square-pulsed operation. Pulse width 1.9×10^{-6} sec. Pulse recurrence frequency 1000 c/s.

electrons is smaller than the maximum attainable (V_a). The placing of the lines, as shown here, — two close together on the "slow" side of the spectrum and one fairly sharp one at the "rapid" side — is found in most cases. Occasionally, however, spectra are found which have one, two or more lines. A continuous background is always present.

Compared with the spectrum of a (BaSr)O-cathode, that of a BaO-cathode is very simple. As with the metallic cathodes, there is only one line and the velocities of the electrons differ only a few eV from the maximum that can be attained. In contrast to this, a SrO-cathode shows a very broad and confused line-spectrum. However, the spectrum of a ThO_2-cathode always consists of one sharp line only.

The influence of the temperature upon the character of the spectra, if any, has not, so far, been considered. *Fig. 9* illustrates the spectra of a (BaSr)O-cathode at different temperatures. It is remarkable that the variation as a function of the temperature shows a maximum. Below 640 °C no velocity spread could be observed; the strongest spread occurred at about 850 °C.

Finally, we have also investigated the relation between the velocity spectrum of the (BaSr)O-cathode and the current density. The results of these measurements have been summarized in *fig. 10*. The potential difference traversed by each group of electrons has been plotted as a function of the total current density. The dotted line indicates the connection between the anode voltage and the total current density.

These curves show that, in general, the velocity spread increases with increasing current density. It is also noticeable that spread occurred with current densities which belong to the extreme left-hand side of the current-density-voltage-characteristic of the diode, in other words, that part where the current is determined by the space charge (also see fig. 1). Conspicuous in fig. 10 is that the (dotted) diode characteristic, once past the saturation area, again curves upwards. This is a phenomenon which has been observed before with oxide-coated cathodes for pulsed operation (abnormal Schottky-effect). In this part of the characteristic the cathode is heated most.

This summary of so many uncorrelated facts is perhaps confusing. Unfortunately it is not possible

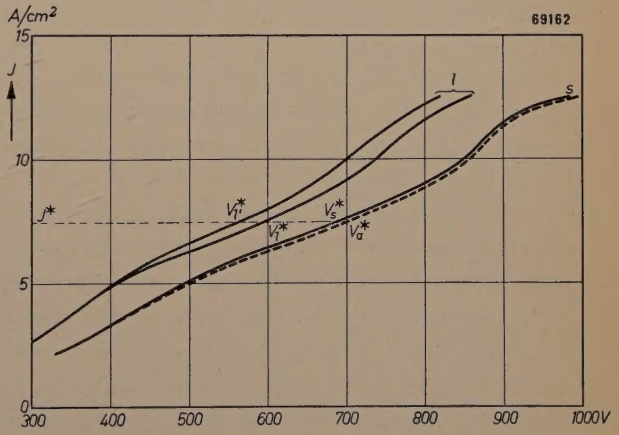

Fig. 10. Current-density-voltage-characteristics for the different electron groups of a (BaSr)O-cathode at a temperature of 840 °C. The voltage difference traversed by each group of electrons is plotted as a function of the total current density. *l* "slow lines", *s* "rapid line". The broken line represents the anode voltage as a function of the total current density. The line is, therefore, the normal diode characteristic. The graph must be read as follows (note the points indicated in the figure): at a current density J^* and an anode voltage V_a^* the spectrum shows groups of electrons with velocities (in eV): $V_{l'}^*$, V_l^*, V_s^*.

to form a theoretical picture which will coordinate all the phenomena discovered into a form which is easy to understand. It is possible, however, to explain some of the phenomena. With regard to other phenomena it will be possible only to make a few observations which serve merely to indicate the direction in which the possible explanation lies.

Possible explanation of the phenomena discovered

In the first place we must try to understand what causes a (BaSr)O-cathode to have a resistance layer at its surface during a current pulse. There is evidence enough to assume that the occurrence of a resistance layer is closely related to the mechanism that is responsible for the conduction of the electrons in the oxide coating [7]). In another article [8]), the two processes which play a part in electron conduction have been extensively discussed. These are:

1. the conduction through the grains of the oxide material;
2. the conduction through the pores between the grains.

The potential which will be found at the outside layer of the oxide coating depends upon the relative contributions of the two mechanisms to the conductivity. This should be seen as follows: First of all assume that there is no conduction through the grains at all and that the electrons in a pore adjacent to the outside layer originate exclusively from the surrounding grains. By applying a difference in potential between the cathode and anode, all the electrons will then be drawn out of this pore. Thus, at that moment, there is no longer pore conduction. (It can be calculated that the time necessary to empty a pore is very much smaller than the duration of a voltage pulse.) Electrons will continue to flow as a result of emission from surface grains until the grains under consideration reach anode potential, thus there will exist a large potential drop in the surface layer. There is, however, conduction through the grains as well as residual conduction through the pores, so that the potential of the outside grains which actually occurs will be between that of the anode and that of the cathode. In cases in which the pore conduction plays no great part, the potential gradient in the oxide coating will be equal to that in a normal resistance. No great potential drop will take place, in that case, at the surface of the oxide coating.

This argument, which holds that the relative importance of the pore conduction determines the magnitude of the potential drop and hence also the extent of the velocity spread, is supported by the following facts, It is known that (BaSr)O, which shows a great velocity spread, has a relatively high pore conduction. In the case of ThO_2, for which only one "line" was found, it can be shown that pore conduction is negligible.

This explains that in (BaSr)O no abnormal velocity spread was observed (see fig. 9*a*) at low temperatures (for example 650 °C). For, at this temperature, the pore conduction is negligible also for this oxide. When the temperature increases, the pore conduction becomes increasingly important, up to a certain limit, because the emission increases more with increasing temperature than the conductivity of the grains. This also actuates the mechanism which originates the potential drop. A further increase in temperature causes, at constant anode potential V_a, a space charge in front of the cathode which limits an increase of the emission at increasing temperature. As the conductivity of the solid material continues to increase, however, the velocity spread of the electrons will diminish in the end.

Although this has given us an idea of the mechanism which causes the large velocity spreads, it is much more difficult to understand why the velocity spectrum is discrete instead of continuous. A definite explanation cannot be given. One of the ways in which the lines of the discrete spectrum might have been caused is as follows :

The electrons with velocities corresponding to the "fastest" line might be emitted from grains which are situated so deeply inside the coating that the conduction is no longer disturbed by the emission, as is the case with the grains in the outer layer (see *fig. 11*). The potential difference of these grains in relation to the metal base is determined only by the total conduction of the oxide and by the current density and one spectral line is obtained.

The fact that the slow electrons are also grouped in "lines" can only be explained by assuming that the ratio between residual conduction and emission is approximately equal for all grains situated in such a way that they can charge themselves.

The occurrence of two "slow" lines indicates that two kinds of electrons are emitted from the charged grains. Superficially one might suppose that these are thermal and secondary electrons. It would be easy for secondary electrons to be formed because the rapid electrons between the grains (emitted from the more deeply situated grains) would liberate secondary electrons through collision.

The explanation given is not, however, conclusive, because the initial velocity of thermal and secondary

---

[7]) R. Loosjes and C. G. J. Jansen, Le Vide, 7, 1131, 1952.

[8]) R. Loosjes and H. J. Vink, Philips Techn. Rev. 11, 271, 1949, 1950.

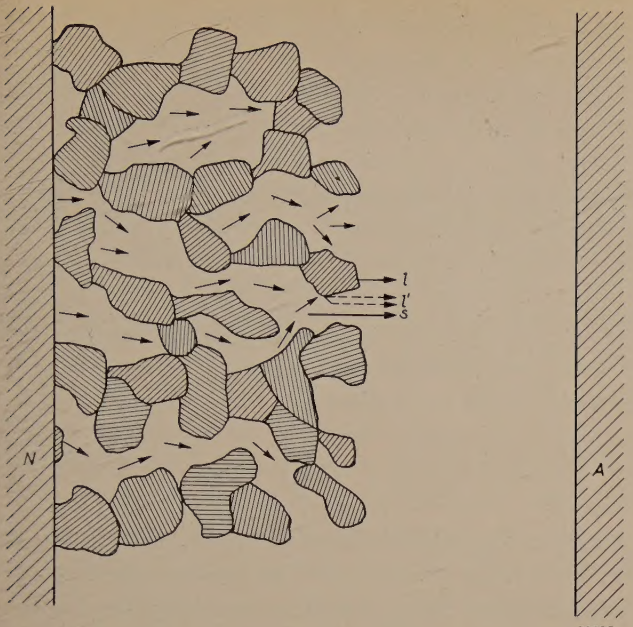

Fig. 11. Cross-section through an oxide coating. Because of the porous structure of the oxide coating the emitted electrons may be divided into: *l* slow thermal electrons, *s* rapid thermal electrons, *l'* slow secondary (?) electrons.

electrons does not differ so much as to be solely responsible for the difference in energy of the two "slow' lines (sometimes some tens of eV).

Consequences of the results found

The existence of a layer with large resistance at the surface of an oxide-coated cathode has all kinds of consequences in practice.

In the first place, the heat development due to the passage of current through the oxide coating, will, for the greater part, occur in the outer layer. As this outer layer has a comparatively bad thermal contact with the vicinity, the temperature increase must be considerable in this region.

The large potential gradient in the outer layer of the oxide coating may also directly influence the behaviour of the cathode. If we assume that the potential changes 200 V within a trajectory of 10 μ (i.e. within a layer having a thickness of only a few grains), a field of 2×10^5 V/cm will be present in this area. It is conceivable that slightly larger field strengths might cause a breakdown in the outer layer (which moreover also has a high temperature). Such a breakdown might start sparking between cathode and anode. This fits in with the fact that ThO_2, which, as we saw, gives no indication of a surface charge, is known to be an emitting oxide in which no sparking phenomena occur. As can be seen from fig. 8*c*, there is no charging of the outer layer with BaO. It is, indeed, a fact that the voltage necessary to produce a spark between cathode and anode is 2 to 3 times as large as that necessary for (BaSr)O and SrO 9).

The occurrence of a velocity spread of the electrons which is caused by the existence of the resistance layer, also affects the behaviour of the cathode. For, if there is a space charge in front of the cathode, this will influence electrons with different velocities in different ways. The fast electrons will be able to penetrate practically untrammelled through the space-charge electron sheath. Thus, the current caused by the rapid electrons will be saturated and become larger only when the temperature is raised. Of the slow electrons, however, only a part will be able to penetrate the space-charge electron sheath. The current caused by these electrons is not saturated and is determined by the space charge. The current contribution of the different lines was measured by means of a tube in which a collector had been incorporated in front of the fluorescent screen. The above-mentioned saturation and space-charge character of the two electron groups was confirmed by the behaviour of the currents determined in this manner, when the anode voltage was increased. As a result of the existence of these groups, the *J*-*V* characteristic of a diode with an oxide-coated cathode ((BaSr)O) must deviate from the characteristic $(J \sim V^{3/2})$, according to Langmuir-Child's formula.

Finally, it should be stated that when our system of measuring was applied to D.C. operation, no abnormal velocity spread 10) was found.

Summary. Following a short summary of the results of former investigations in the sphere of thermionic emitters under pulsed conditions, a more detailed description is given of investigations in this sphere made by the authors. The potential gradient in the oxide coating of a cathode for pulsed operation was first investigated. This indicated that the layer with large resistance in the interface between nickel and oxide, often encountered by other investigators, was absent in the cathodes investigated by us. It appears, however, that in the case of some oxide-coated cathodes, such as (BaSr)O and SrO, a layer with large resistance occurs at the side nearest the anode, which results in a considerable increase in potential in the outer layer of the oxide coating. This, in turn, causes a large velocity spread of the emitted electrons which often amounts to hundreds of electron volts. By means of a specially constructed tube, the velocity spectrum was examined for different kinds of cathodes under different conditions. The spectrum, curiously enough, appeared to be discrete. The occurrence of the layer with large resistance, which results in the considerable velocity spread, is probably due to two mechanisms causing the conduction through the oxide coating: the pore conduction and the conduction of the grains of the oxide. The relative importance of the two conduction mechanisms will have a decisive influence on whether the layer of large resistance occurs or not. No satisfactory explanation has been given so far for the occurrence of discrete lines in a velocity spectrum. The considerable potential gradient in the outer layer of the oxide may well be one of the causes of the sparking observed with oxide cathodes under pulsed conditions.

---

9) E. A. Coomes, J. appl. Phys. **17**, 446, 1946.

10) During D.C. operation abnormal spread was found only in the case of SrO cathodes. For further investigations in this field the reader is referred to the work by G.C. Dalman, Report R 224-49, Polyt. Inst. Brooklyn 169, New York 1949.

NEW PHOSPHORS FOR FLUORESCENT LAMPS

by J. L. OUWELTJES.

621.327.43:546.411.85:535.625

The demand for suitable phosphors for fluorescent lamps has led to widespread research during the last few years. Until recently, it was necessary to mix two or more phosphors in order to obtain white fluorescent light, but the discovery of halophosphate phosphors has made it possible to obtain white light with only one phosphor. This is a great asset in the manufacture of fluorescent lamps, and, moreover, halophosphates have a higher efficiency and are better able to withstand the effects of mercury vapour. If a more faithful rendering of red is desired, magnesium-arsenate, which emits red light, can be mixed with the halophosphate. The spectral distribution of this combination very closely approximates to that of a black body.

Introduction

Tubular fluorescent lamps contain a filling of mercury vapour at low pressure. Under the influence of an electric discharge, this vapour emits radiation which is for the greater part concentrated in several spectral lines in the ultra-violet part of the spectrum, with about 80% in the resonance line at $\lambda = 253.7$ mμ. In order to convert this radiation into visible light, the interior of the tube is coated with a fluorescent substance (a phosphor) which emits visible light rays when subjected to the ultra-violet irradiation. The spectral distribution of this light as well as the efficiency with which the electric power is converted into light are wholly dependent on the composition and properties of the phosphor. To obtain maximum efficiency, the phosphor must absorb all the ultra-violet rays, and emit a quantum of visible light for every quantum of ultra-violet absorbed (quantum efficiency 100%).

In order that the lamp shall function as a useful light source, the spectral distribution should as nearly as possible meet a number of requirements, the most important of which are as follows:

1) The light emitted should be white. This means that an object with a coefficient of reflection which, in the visible spectrum, is independent of wavelenght, should appear to the eye as white when illuminated by the lamp, i.e. the visual impression should correspond to that obtained in daylight.
2) Good colour rendering. When an object having a coefficient of reflection that is dependent on the wavelength is illuminated by the lamp, the object must appear to the eye to be of the same colour as when it is irradiated by a black body of the same colour temperature as that of the lamp.

In order to satisfy the requirements concerning efficiency and spectral distribution, it has until recently been common practice to coat the tube with a mixture of phosphors, viz. zinc-beryllium silicate and magnesium tungstate. The spectral distribution of neither of these phosphors even approaches the ideal, but when the two are mixed, the resultant spectral distribution, being the sum of the two single distributions, is well within the limits imposed. The efficiency of the mixture is also satisfactory.

For the lamp manufacturer, however, the necessity of having to use a mixture of two phosphors is in some respects a drawback. It is often difficult to produce the exact colour required, since differences in the grain size and compositon of the constituents, and consequent variations in the efficiency of the two phosphors, are practically unavoidable. These variations lead to displacements in the colour value.

The search for a single phosphor which would emit light with a spectral distribution conforming to the above requirements, was instigated in order to obviate these difficulties. Some years ago, a group of such phosphors, namely the halophosphates were discovered ¹). As a result of this discovery, it is now possible to prepare white-fluorescent single phosphors in great variety, and, although the compositions of these phosphors may vary slightly, the basic constituent is always the same. It is possible to produce with these phosphors the colours of all present-day fluorescent lamps, ranging from "cold" daylight (colour temperature 6500 °K) to the "warm" colours (3000 °K). The demand for a single phosphor capable of emitting white light has thus been amply met.

In addition to the advantages of halophosphates already mentioned, the efficiency of these substances is greater than that of the silicate-tungstate mixture. Furthermore, they are better able to withstand the effects of mercury vapour, and partly because they absorb little of the vapour, this being a drawback

---

¹) H. G. Jenkins, A. H. Mc Keag and P. W. Ranby J. Electrochem. Soc. 96, 1-12, 1949.

which renders many other phosphors unsuitable for fluorescent lamps. As a consequence a lamp coated with halophosphate phosphor retains more of its good properties toward the end of its life than does a silicate-tungstate lamp.

It is a remarkable fact that the development which followed the discovery of the halophosphates ultimately produced an entirely new range of lamps coated with phosphor mixtures even more complex than those previously used. This development was founded on the second requirement imposed on the spectral distribution of the light source, viz. good colour-rendering. In those cases where good colour rendering is not of primary importance, e.g. in street- and workshop lighting, the halophosphates are excellent, but if true colour rendering is desired, particularly in the red region, a phosphor with red fluorescence must be added. In this case, too, the new phosphors are, however, still to be recommended, since they give a better colour rendering than silicate-tungstate mixtures.

In this article, a discussion of the properties of the halophosphates is followed by a description of the method employed to improve the colour rendering.

Fluorescence with ultra-violet irradiation

As already mentioned, a mixture of zinc-beryllium silicate (activated with manganese) and magnesium-tungstate has hitherto been used in most fluorescent lamps. The colour of the fluorescence of silicate irradiated with ultra-violet light (mercury line $\lambda = 253.7$ mμ) is yellow, that of the tungstate blue. *Fig. 1* shows the spectral energy distribution of the individual phosphors, together with that of the mixture normally used.

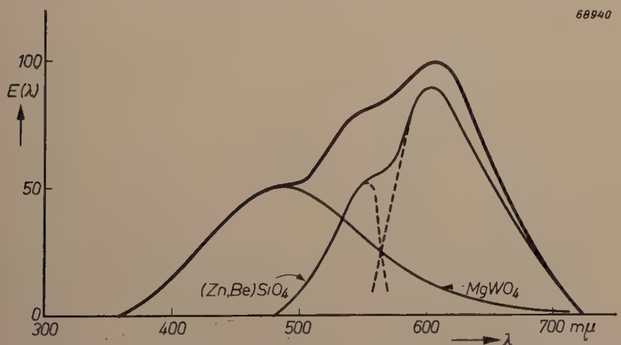

Fig. 1. Spectral energy distribution of $(Zn,Be)_2SiO_4$, activated with Mn (yellow fluorescence), and that of $MgWO_4$ (blue fluorescence) (thin lines). The curve relating to $MgWO_4$ is flat-topped at $\lambda = 480$ mμ (in the blue-green region), whereas the other curve has its major peak at $\lambda = 610$ mμ (orange) and a smaller peak at $\lambda = 560$ mμ. The emission of the silicate actually consists of two emission bands (dotted lines). The heavy line represents the total energy distribution of the mixture generally used in practice, comprising two individual components. The energy is plotted on a relative scale.

Since the mechanism of fluorescence has already been fully discussed in this journal[2]), a brief summary will now suffice. When a substance such as zinc-beryllium silicate containing a small quantity of manganese is irradiated by ultra-violet rays of the wavelength $\lambda = 253.7$ mμ, much of this radiation is absorbed: due to the incorporation of manganese atoms, the crystal lattice absorbs the energy of many radiation quanta. Part of this energy is converted into lattice vibration energy, that is, into heat; in the instance under discussion, however, by far the greater part of the energy is again transferred from the crystal lattice to the manganese atoms, which are thus excited. This state of excitation lasts only a very short time. After this period the atom emits rays of visible wavelength, mainly in the region of $\lambda = 600$ mμ, i.e. in the orange region. This fluorescence radiation is therefore brought about entirely by the manganese atoms in the crystal lattice, for which reason these atoms are known as activating atoms, or activators.

The fluorescence of magnesium tungstate takes place without the presence of any activators; the WO_4 ions function as selective absorption centres which are excited when rays of a given wavelength reach the crystal. When these ions return to their original level, which they do in stages, a radiation quantum of greater wavelength, mainly in the blue-green region, is emitted.

We shall confine ourselves to this simple description of the mechanism of fluorescence, without touching upon the complications which frequently occur.

Generally speaking, the fluorescence of phosphors, apart from that of the comparatively rare substances which require no activator, is governed mainly by the nature and concentration of the activating atoms, and by the manner in which these atoms are incorporated in the crystal lattice.

Let us consider the fluorescence of zinc-beryllium silicate more closely: it appears that there are actually two "emission bands" (see dotted lines in fig. 1) which together form a single, less sharply defined band with a hump on one side. It is therefore assumed that there are two categories of activating atoms which differ, for example, in the manner in which they are surrounded by the other atoms.

With this in view, an attempt might be made to evolve a phosphor which would emit white light without the addition of any other phosphors, by introducing activating atoms into a substance in a way such that the various emission bands will combine to produce white light. This is not actually practicable, however, but it is possible to obtain the same effect by introducing two (or more) different activators into a single parent crystal, one activator giving, for example, yellow fluorescence and the other blue.

---

[2]) See, for example, F. A. Kröger and W. de Groot, The influence of temperature on the fluorescence of solids, Philips Techn. Rev. **12**, 6-14, 1950/1951 (No. 1).

The halophosphates

Halophosphates constitute a group of substances which permit of the interposition of two activators. The crystal lattice and composition of halophosphates are closely related to those of the natural mineral apatite. The chemical formula of pure fluor-apatite is $3Ca_3(PO_4)_2.CaF_2$. From a stoechiometrical point of view, the molecule is, therefore, built up of 3 calcium phosphate molecules and 1 calcium fluoride molecule. The fluorine is sometimes completely or partly replaced by another halogen, say chlorine, whilst the calcium atoms can be replaced, also wholly or in part, by other bivalent metals (e.g. cadmium, iron, magnesium). It is even possible to incorporate an OH^--group, a CO_3^{2-}-group or an SO_4^{2-}-group instead of halogen ions, whilst trivalent rare earths may be substituted for the metal atoms.

In halophosphate phosphors producing white light, a small proportion of the calcium ions has been replaced by trivalent antimony ions and bivalent manganese ions, both of which are activators, the antimony ions giving fluorescence in the blue emission band and the manganese producing a yellow band. Some of the fluorine ions are replaced by chlorine ions.

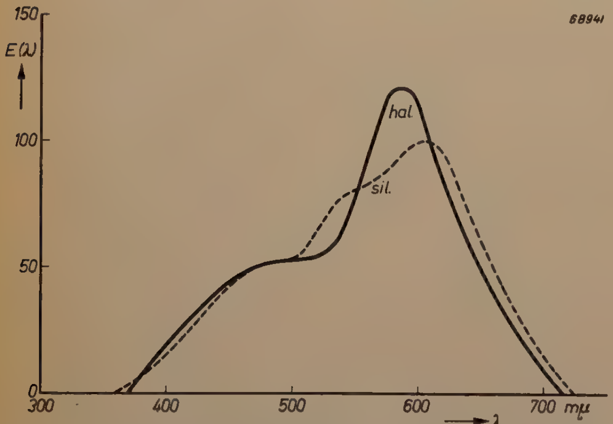

Fig. 2. Spectral energy distribution of a halophosphate phosphor activated with antimony and manganese. The blue antimony band with a peak at $\lambda = 475$ mμ is readily distinguished from the yellow, manganese band with a maximum at $\lambda = 590$ mμ. For comparison, the spectral energy distribution of a silicate-tungstate mixture (fig. 1) is shown (broken line). The halophosphate produces more yellow light, but less green and red. Energies are again plotted on a relative scale; the areas enclosed by the two curves are equal.

Fig. 2 shows the spectral energy distribution of a certain halophosphate phosphor (heavy line). The blue emission band, with a peak at $\lambda = 475$ mμ, is clearly distinguishable from the yellow emission band which peaks at $\lambda = 590$ mμ. The actual location of each band and the height of the peaks appear to be dependent on the composition of the phosphor. The blue (antimony) band shows a maximum at $\lambda = 475$ mμ, the location of this maximum being almost independent of the composition, whereas that of the yellow (manganese) band is governed mainly by the ratio of chlorine-to-fluorine in the crystal: the greater the quantity of fluorine replaced by the chlorine, the longer the wavelength at which the maximum occurs. Moreover, the quantity of manganese introduced to obtain emission also affects the position of this band.

It is assumed that both antimony and manganese ions replace those Ca^{2+}ions which are in the vicinity of halogen ions. When an Sb^{3+} ion is incorporated, the adjacent halogen ion is replaced by an O^{2-}ion in order to maintain electric neutrality. The Sb ions are not, therefore, in direct contact with the halogen ions, and the substitution of chlorine for fluorine will have little effect on the excitation of the antimony. On the other hand, bivalent manganese ions are in the vicinity of halogen ions, and the emissivity of the manganese is definitely affected by the substitution of fluorine by chlorine.

The intensity ratio of the emission is determined mainly by the quantity of manganese present in the phosphor. It is possibly surprising to note that the quantity of antimony introduced has no effect on this ratio (although it does, naturally, affect the absolute heights of the maxima). To explain this, it must be assumed that the excitation of manganese ions is not the direct result of ultra-violet irradiation, but the indirect result of the transfer of part of the excitation energy from antimony ions to manganese ions. This is usually expressed by stating that the antimony ions are not only activators, but also sensitizers for emission by the manganese. The fraction of excitation energy transferred from Sb ions to Mn ions is dependent only on the number of Mn ions available, i.e. on the manganese concentration. This, then determines the intensity ratio of the emission bands.

The hypothesis relating to the transfer of energy is confirmed by the following: A halophosphate to which only antimony is added gives blue antimony fluorescence when subject to radiation of wavelength 253.7 mμ, but a halophosphate containing only manganese emits no light at all when thus irradiated. The manner in which energy is transferred from Sb to Mn cannot be dealt with here.

Colour and colour rendering of halophosphate phosphors

According to the foregoing, the white fluorescence of a halophosphate activated with antimony and manganese is a result of the superimposition of the blue fluorescence of antimony on the yellow of the manganese. The colour of the resultant light can be controlled to some degree by varying the quantity of manganese added (since this determines the position of the yellow emission band, and the intensity ratio of this band to the other) and, to a lesser degree, by varying the chlorine-to-fluorine ratio: by increasing the chlorine content the wavelength of the yellow emission band is increased and in consequence the total spectral distribution is displaced towards the red zone. The result of the two effects can best be illustrated with reference to the colour triangle [3]).

Any change in the composition of the phosphor will produce a change in the colour of the light emitted, which means that the relevant colour point in the colour triangle is displaced. This is illustrated in *fig. 3*, where the curved line *BGR* represents the spectral colours, the straight line *BR* being the so-called purple line connecting the two colour points extreme red and extreme blue. Curve *b* is the "black-body" line, indicating the position of the colour point of the black body as a function of the absolute temperature (a few of the values are shown). The colour point of daylight corresponds roughly to that of a black body at 6500 °K.

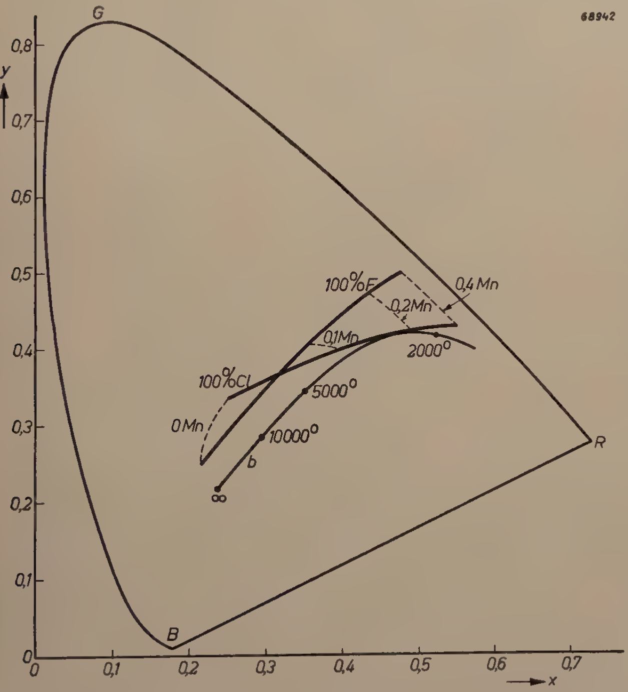

Fig. 3. Colour triangle on *x-y* co-ordinates. The curve *BGR* represents the spectral colours; *BR* is the purple line, whilst line *b* connects the colour points of black-body radiation at various absolute temperatures. A few of the temperatures are indicated (daylight corresponds roughly to black-body radiation of 6500 °K). The thick lines show the displacement of the colour point of a halophosphate phosphor when the Mn content of the phosphor, which contains a given quantity of fluorine-chlorine, is varied. The manganese content is indicated by the number of Mn atoms per calcium-halophosphate molecule specified on the broken lines. The lines representing constant halogen ratios are almost parallel to the black-body line. (Derived, in part, from K. H. Butler and C. W. Jerome, J. Electrochem. Soc. **97**, 265-270, 1950 (No. 9).

Any change in the Mn-content of the phosphor has the effect of displacing the colour point of the fluorescent light along a line almost parallel to the black-body line (see thick lines in fig. 3). At the same time, the actual "path" of the colour point is also slightly dependent on the fluorine-chlorine content. With a given Mn-content, the colour point almost describes a straight line when the fluorine-chlorine content is varied, the angle of the path being governed once again by the Mn-content (see broken lines).

Although the position of the colour point is sufficient indication of the colour of the light, the colour rendering cannot be assessed without a more or less comprehensive survey of the spectral distribution of the emission. Let us compare the colour rendering of a new halophosphate lamp with that of the old type silicate-tungstate lamp. The *table* on the next page contains details of the spectral distribution of a "white" silicate-tungstate lamp the colour temperature of which is 4000 °K (line 1) and that of a "white" halophosphate lamp with a colour temperature of 4200 °K (line 2). The halophosphate lamp is designed to replace the silicate-tungstate lamp; the difference in colour temperature is the outcome of international standardization. Also included in the table are data relating to black-body radiation (line 4) with a colour temperature of 4000 °K, and particulars of another new lamp which will be discussed later. Those spectral regions have been chosen [4]) which will give a representative impression of the colour rendering; the components of the luminous flux are shown as relative quantities (percentages), the total quantity of light emitted by each lamp over the entire spectrum being taken as 100.

According to the data in the table, the agreement between halophosphate and the black body is not so good as that between silicate-tungstate and the black body. This in understood on comparing the

---

[3]) See W. de Groot and A. A. Kruithof, The colour triangle, Philips Techn. Rev. **12**, 137-144, 1950/1951 (No. 5).

[4]) See P. J. Bouma, The colour reproduction in the use of different sources of "white" light, Philips Techn. Rev. **2**, 1-7, 1937.

Percentage of luminous flux contributions in 8 spectral regions of a lamp with (1) white-fluorescent silicate-tungstate coating: white silicate lamp, colour temperature 4000 °K, (2) white-fluorescent halophosphate coating: "standard" type, colour temperature 4200 °K, (3) white-fluorescent mixture comprising halophosphate and magnesium-arsenate (plus a small quantity of willemite): "de Luxe" lamp, colour temperature 4200 °K. The values on line 4 represent the spectral distribution of a black-body at a colour temperature of 4000 °K. The colour matching of any two lamps is practically identical when the luminous flux of the one lamp does not differ from that of the other by more than 25% in any one of the eight columns.

Wavelength range (mμ)	380-420	420-440	440-460	460-510	510-560	560-610	610-660	660-760
Light source	violet	blue-violet	blue	green-blue	green	yellow	orange	red
1) White silicate lamp	0.010	0.35	0.30	4.80	38.0	43.0	13.0	0.43
2) "Standard" lamp	0.012	0.335	0.405	6.00	35.5	49.0	8.4	0.20
3) White "de Luxe" lamp	0.010	0.32	0.29	4.93	40.1	41.4	12.3	0.65
4) Black-body 4000 °K	0.014	0.13	0.47	7.89	38.0	39.5	12.9	1.05

spectral energy distributions of the two phosphors. To facilitate this comparison, the spectral energy distribution curve of the silicate-tungstate phosphor in lamp 1 is shown in Fig. 2 (broken line). In the yellow region, the halophosphate curve has a higher peak than the curve of the mixture, but, on the other hand, the phosphate emission contains less green and, more particularly, less red. On considering lines 2 and 4 more closely, we see that the difference in the spectral distribution of the halophosphate and the black body is manifested mainly in the last two columns, i.e. in the red. The differences in the first four columns (blue) are due chiefly to the previously mentioned difference in colour temperature, and are therefore unimportant.

It follows from the above, then, that the halophosphates give insufficient red light, the most noticeable result of this being that red and pink objects (the colour of the skin) appear in an unnatural brownish, deathly tinge.

This can be remedied to some extent by reducing the fluorine : chlorine ratio (see fig. 3), as the Mn content exceeds one-tenth per molecule. The Mn-content cannot be increased, seeing that this would affect the colour temperature, The increase in the chlorine content results in a displacement of the colour point towards the purple line. Even so, red objects would not appear entirely natural. This is not objectionable for many practical applications.

This procedure was adopted to produce the "standard" type of lamp intended for industrial purposes, street lighting, etc. Compared with a silicate-tungstate lamp, the new lamp has three distinct advantages: namely only one phosphor is required in manufacture, the efficiency is higher, and the characteristics of the lamp towards the end of its effective life show a distinct improvement.

Improvement of colour rendering: the "de Luxe" lamp

In all cases where good colour rendering is of the first importance, the "standard" lamp is unsuitable. This difficulty could be overcome by reverting to silicate lamps, but in view of the lower efficiency and poorer maintenance of these lamps, it is worth while to seek to improve the colour matching properties of the halophosphate lamp. Theoretically, this can always be achieved by adding a red fluorescent substance to the white, although the principal advantage of the halophosphate lamp is then of course lost. The efficiency, too, decreases slightly when a red phosphor is added to a halophosphate: this is unavoidable since the eye is less sensitive to red than to yellow or green. On the other hand, if a red phosphor with a quantum efficiency approaching 100% and suitable spectral distribution were available, this phosphor could be mixed with halophosphate to produce a lamp having much better matching properties than a silicate-tungstate lamp with almost the same efficiency. Such a phosphor, in the form of magnesium arsenate, was actually discovered; this is a fluorescent substance having a deep red emission and the highest quantum efficiency of all known red fluorescent substances (85%). Magnesium-arsenate has already been mentioned in a previous article ⁵) (in this article the quantum efficiency is given as 75%, but recent samples showed an efficiency 10% higher).

Apart from the high quantum efficiency of magnesium-arsenate, there are two other factors to which the high efficiency of lamps using this phosphor is attributable, viz:

---

⁵) J. L. Ouweltjes, W. Elenbaas and K. R. Labberté, A new high-pressure mercury lamp with fluorescent bulb, Philips Techn. Rev. 13, 109-118, 1951/1952 (No. 5).

a) This phosphor responds to the entire ultraviolet spectrum (and part of the blue spectrum) of the low-pressure mercury discharge. This spectrum consists not only of the resonance line at $\lambda = 253.7$ mμ, but also lines at $\lambda = 313$ mμ, $\lambda = 365$ mμ, etc., with a weak, continuous background. Halophosphates, as well as silicates and tungstates, are excited by the resonance line only. When magnesium arsenate is added, some of the previously unused rays are utilized and, moreover, part of the visible blue light emitted by the mercury vapour, mainly in the spectral line $\lambda = 436$ mμ, is absorbed by the arsenate, resulting in a slightly better rendering of blues and yellows.

b) Magnesium-arsenate has a very sharply defined emission band (see fig. 5 in the article quoted in footnote [5]); in contrast with other phosphors emitting red light, magnesium-arsenate emits no infrared.

Halophosphate fluorescence is lacking not only in red light, but also, to a lesser extent, in green. For this reason a small quantity of willemite (zinc silicate) emitting green radiation is added. In this way, the colour matching is improved without displacement of the colour point.

This development has led to an entirely new type of lamp, namely the "de Luxe" lamp. Although the advantage of a single phosphor is no longer applicable (a mixture comprising three phosphors is used), the colour matching properties compare very favourably with those of the silicate-tungstate lamp. The spectral distribution of the white "de Luxe" lamp with a colour temperature of 4200 °K ("warm-white" and "daylight" lamps are also available) is given in the table (line 3); the values correspond very closely to those of a black body with radiations of roughly the same colour temperature (line 4). This is also apparent in fig. 4, in which the spectral energy distribution of the lamp and that of the black body are reproduced.

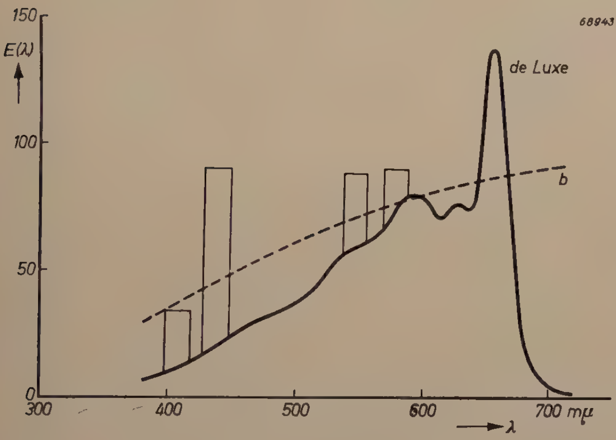

Fig. 4. Relative spectral energy distribution of the "white" "de Luxe" lamp with a colour temperature of 4200 °K (fully drawn line) compared with that of a black body with a colour temperature of 4000 °K (broken line). Superimposed on the fluorescent light are a few spectral lines emitted by the mercury vapour.

Summary. A light source for general lighting purposes must meet certain requirements as regards colour and spectral distribution of the light emitted (colour rendering). Until recently, low-pressure fluorescent lamps have fulfilled these requirements if coated with a mixture of two phosphors, zinc-beryllium silicate and magnesium-tungstate. To avoid the difficulties entailed by the use of such a mixture in the manufacture of fluorescent lamps, a phosphor was sought which would by itself emit white light. Phosphors having this property were discovered in the halophosphate group; these phosphors contain two kinds of activating atoms; the one, antimony, emits blue light and the other, manganese, yellow. The spectral distribution and the colour triangle are used as basis for determining the colour and matching properties of the phosphors, respectively. It appears that some control can be effected by varying the composition of the phosphor. The efficiency of fluorescent lamps with halophosphate phosphors is greater than that of lamps coated with the silicate tungstate mixture. In those cases where good colour matching is essential, also in the red region, red-luminescing magnesium arsenate and a small quantity of willemite are mixed with the phosphor. Because of the excellent properties of magnesium arsenate, the efficiency is reduced only slightly by the inclusion of this substance, thus producing a lamp (the new "de Luxe" lamp) which ensures high efficiency and excellent colour matching properties.

AN INDENTATION METER FOR PAINT

by J. HOEKSTRA and J. A. W. van LAAR.

667.6:620.178.152:621.317.39

In all industries in which paints are made or used, the need has long been felt for a means of measuring those characteristics of paints which determine their quality, by a method capable of being accurately reproduced. One of the most important properties of a coat of paint is its resistance to the penetration of hard objects. A method hitherto all too frequently employed to determine this resistance consists in scratching the surface with the finger nail — a "test" which, it is true, yields more information to experienced persons than might be supposed, but which cannot possibly provide a basis for scientific research.

The authors of this article have substituted for the finger nail a sapphire which is specially shaped to give a reproducible impression when applied to a coat of paint. The depth of this impression is measured by an electrical zero method.

The greater the resistance of a coat of paint to damage in the form of indentations, scratches, etc., in other words, the "harder" the paint, the longer it is able to fulfil its task of providing a decorative or protective coating. In order objectively to determine the composition, method of drying, etc. that is most suitable for a given purpose, it must be possible to measure the resistance of the paint to the penetration of hard objects, i.e. the "hardness" of the paint. The lack of a reproducible method of determining this quality more often than not leads only to fruitless argument.

To measure the hardness of a metal, the Brinell, Rockwell or Vickers [1]) method is usually employed. In the Brinell and Vickers tests respectively round and tapered rams of great hardness and standardised dimensions are pressed to the metal with a certain force. When the ram is withdrawn, the superficial area of the indentation thus produced is measured, and the applied force divided by the area then represents the hardness of the metal. It is true that this definition of the hardness is not directly related to purely physical constants, but the tests are fairly easily reproducible and are therefore of great importance from the technological point of view; the quantity thus measured may be termed a "technoligical quantity".

When applied to coats of paint the above methods suffer from the objection that the impression is very often not clearly defined, so that the area of the indentation cannot be measured with any accuracy. Furthermore, when the load is removed, the impression contracts, firstly owing to the not inconsiderable recovery of the elastic part of the deformation and, secondly, as a result of elasto-plastic flowing of the material ("retarded elasticity"), by reason of which the impression shrinks still further, according to the time lapse. Moreover, experiments have proved that in contrast with most metals the area of the indentation in a coat of paint is not proportional to the applied load, so that there is no object in specifying a certain "hardness" value without stating the load.

Principle of the instrument

The method employed by the authors has eliminated the first two objections mentioned above. As in the Vickers test, a hard, pointed ram is pressed against the surface to be tested with suitable force. This ram takes the form of a regular square pyramid having an apex angle of 136°. In this case, however, instead of measuring the dimensions of the resultant impression *in* the plane of the surface *after* removal of the load, the *depth* of the impression is measured *while* the force is *still* being applied, thus eliminating the problem of the vague outline. By again measuring the depth of the impression a certain time after the load is removed it is possible to ascertain roughly the relationship between the plastic and elastic parts of the deformation.

In view of the absence of a proportional relationship between the area (or square of the depth) of the indentation in a coat of paint and the applied force, we give the preference not to computing the "hardness" as such, but to state the depth of the impression (together with the applied force).

As with hardness tests on metals, the depth of the impression is here again in some degree dependent on the time during which the force is actually operative. This is not a drawback from the point of view of the reproducibility of the test, provided that the force is always applied during the same period of time, or at any rate that this duration is indicated in the result. Thirty seconds has been found suitable for tests on most paints, varnishes, lacquers, etc.

---

[1]) See, for example, Philips Techn. Rev. 2, 177-181, 1937.

The force applied to the ram should always be such that the depth of the impression will be small compared with the thickness of the coat of paint. If the point of the sapphire is permitted to penetrate too close to the surface to which the paint is applied, it will reach a zone in which this surface noticeably hinders the yielding of the paint; the value measured then represents an "apparent" hardness which is considerably higher than the much more important value related to the outer surface. Since most coats of paint are not more than 25 to 100 μ thick, the penetration depth must be limited to a few microns, and the measurement must be accurate to within 0.1 μ.

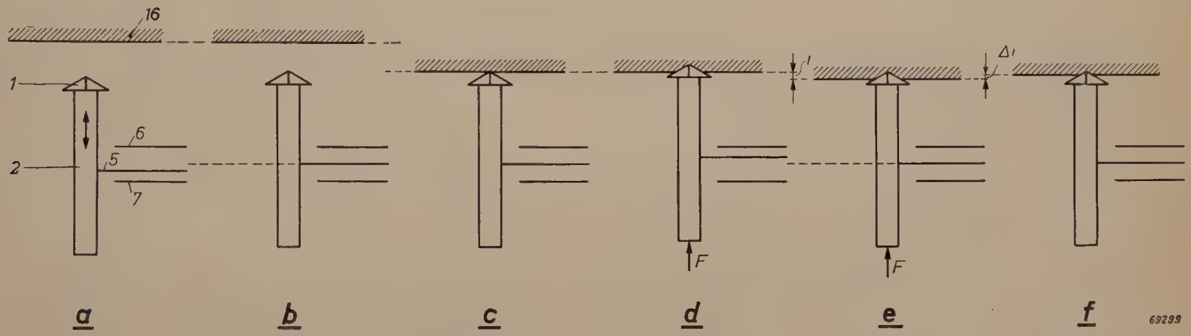

Fig. 1. Diagram showing the principle of the indentation meter: a sapphire *1* is mounted on a ram *2* which is capable of vertical movement and which carries the centre plate *5* of a differential capacitor, *6* and *7* being the fixed plates. The specimen plate with paint *16* can be raised or lowered by means of a micrometer screw (not shown). (The numbers in this diagram correspond to those shown in the other figures.)
a) Starting point (arbitrary position).
b) Plate *5* adjusted centrally between the fixed plates, *6* and *7*.
c) Specimen lowered until it just touches the tip of the sapphire.
d) Force *F* (e.g. 10 g) applied to the ram presses the tip of the sapphire into the paint.
e) Specimen quickly lowered until plate *5* is again central between plates *6* and *7*, cancelling out the upward movement of the ram and restoring the load exactly to 10 g. This downward pressure is maintained for 30 seconds, care being taken that the bridge remains exactly balanced. The difference between the micrometer reading at stage (*c*) and that at the end of the 30-second period then represents the penetration depth *i*.
f) The variation *Δi* in the penetration depth can be determined when the force *F* is withdrawn and balance is restored by adjusting the micrometer screw.

With the instrument described in this article the penetration depth is measured by an electrical zero method. Every movement of the ram is communicated to the centre plate of a differential capacitor of which the other two electrodes are fixed plates (*fig. 1a*). The two halves of this capacitor, together with two identical resistors, form a bridge; an alternating voltage is applied across one diagonal and the voltage across the other is amplified and applied to an indicator. The bridge is in balance when the centre plate of the capacitor is central between the two fixed plates, i.e. when the tip of the sapphire is at a certain level.

The procedure is as follows: The paint is applied to a solid surface (specimen plate); after drying, this plate is clamped to an adjustable platform on the instrument. Before the sapphire is brought into contact with the paint, the control knob of the bridge is set to its centre position and the bridge is roughly balanced by raising or lowering the centre plate of the differential capacitor by means of a set-screw until it is central between the two fixed plates (fig. 1*b*). Exact balance of the bridge is then obtained by carefully acting on the control knob of the bridge, thus compensating slight deviations of the centre plate of the differential capacitor.

The platform holding the specimen plate is now carefully lowered over the sapphire by turning a calibrated micrometer screw until the surface of the paint just touches the tip of the sapphire (fig. 1*c*), this being shown by the indicator which responds immediately as the balance of the bridge is disturbed.

At this stage the reading of the micrometer screw is taken and a certain force, say 10 g, is applied to the ram (fig. 1*d*) — the manner in which this load is applied is described later. The tip of the sapphire is thus forced into the coat of paint. The load is applied for 30 seconds, during which period the bridge is kept in balance by constant adjustment of the micrometer screw, so that the sample is lowered accordingly (fig. 1*e*). During this 30-second period the depth of penetration of the sapphire into the paint will increase to some extent, but the position of the ram with respect to the fixed parts of the instrument remains unchanged. At the end of this period, a second reading is taken from the scale on the micrometer screw, the difference between this reading and the first being the depth *i* to which the sapphire has penetrated into the paint.

If so desired, the load can be removed immediately after the second reading has been taken. Then, after a definite time, the bridge is again balanced by readjusting the micrometer screw (fig. 1*f*), and another reading is taken. The difference Δi between the second and third readings gives us the residual, irrevocable penetration depth which, as already mentioned, furnishes an indication of the relationship between the elastic and plastic properties of the specimen.

Construction

The first idea for this penetration meter dates back to 1942, but since then the original design has been improved in many ways. Disregarding the now obsolete models which have been reported else where [2] [3], we shall now describe only the most recent model (*fig. 2*) which is in use in many departments of the Philips factories [4].

Fig. 3 depicts a vertical cross section of the instrument: *1* is the sapphire for producing the indentation. In the Vickers test a diamond is used, but for paints a sapphire ground to the shape of the Vickers diamond (a square pyramid having an apex angle of 136°) is sufficiently hard. This sapphire is mounted in a metal sleeve at the upper end of the ram, which is held in place by two flat springs. Also attached to this ram, but insulated from it, is the movable plate of the capacitor, measuring approximately 4 cm × 5 cm. Since the gap between the movable plate and each of the fixed plates is only about 50 μ, it is essential that the fixed plates be held securely in place and they are therefore supported by sturdy porcelain rods, cemented in place. As the ram is held in position by two flat springs, movement of the centre plate is restricted to parallel displacement.

Each of the three plates of the capacitor is wired to a plug pin for connection to a "Philoscope" bridge, type GM 4144 [5]) which contains all the other components required to form a complete bridge circuit, viz. the two resistance arms, an amplifier, an electronic indicator ("magic eye") and a power unit.

A weak spring in the form of a thin, steel wire (*13* in fig. 3) is secured to the ram holding the sapphire, and, by adjusting a set-screw *14*, which controls this spring, the movable plate of the capacitor can be brought roughly midway between the fixed plates (fig. 1*b*). The exact balancing of the bridge is easily done by electrical adjustment. The bridge must be balanced before every measurement, but as a rule readjustment of the bridge resistors suffices.

The sapphire passes through a hole in a platform *15*, to which the specimen is clamped, painted side down. This platform can be raised or lowered by means of a micrometer screw *18*, which, to ensure maximum accuracy, actuates the platform, not direct, but through reducing gear of 1 in 50.

This mechanism is depicted in *fig. 4*. One end of the platform *15* (the right-hand end in figs 3 and 4) is fixed to the framework *20* of the instrument by means of a flat spring *19*. A beam *21* is also mounted on the framework, by means of a flat spring *22*, and the end of an adjustable screw *23*, protruding from the platform, rests on this support. It will be seen from fig. 4 that any displacement of the micrometer screw, reduced by a factor of $(l_2/l_1) \times (l_4/l_3)$, is transmitted to the platform with respect to the sapphire. The lengths l_1, l_2, l_3 and l_4 are such that this factor is exactly 50.

Screw *23* serves to lower the platform until the top is about

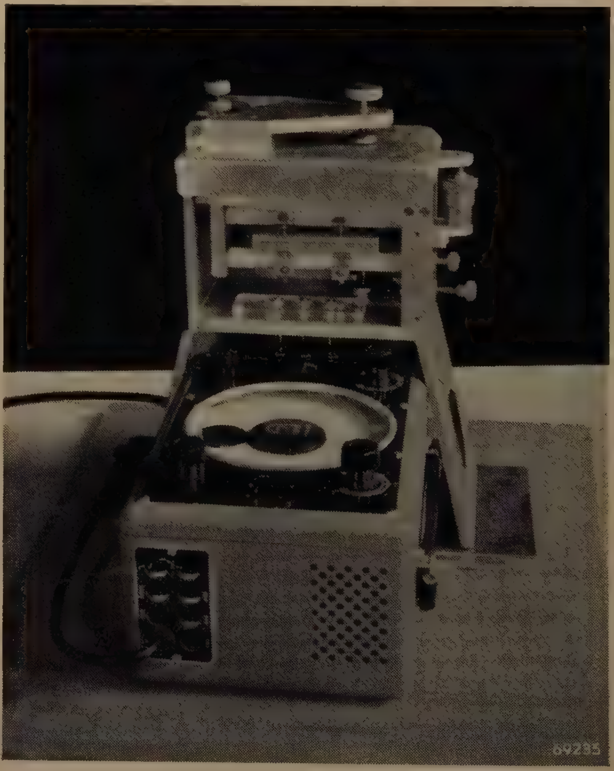

Fig. 2. Indentation meter with "Philoscope" in the foreground.

---

[2]) J. Hoekstra, The hardness of paints (in Dutch), Verfkroniek **19**, 88-90, 1946.

[3]) J. Hoekstra and H. A. W. Nijveld, The determination of the hardness of organic films, Rec. Trav. chim. Pays-Bas **67**, 685-689, 1948.

[4]) Credit for some of the constructional details is due to the Central Workshop of the Research Lab. Eindhoven, and, more particularly, to Mr. J. M. van Ostade.

[5]) An older type (GM 4140) is described in Philips Techn. Rev. **2**, 270-275, 1937.

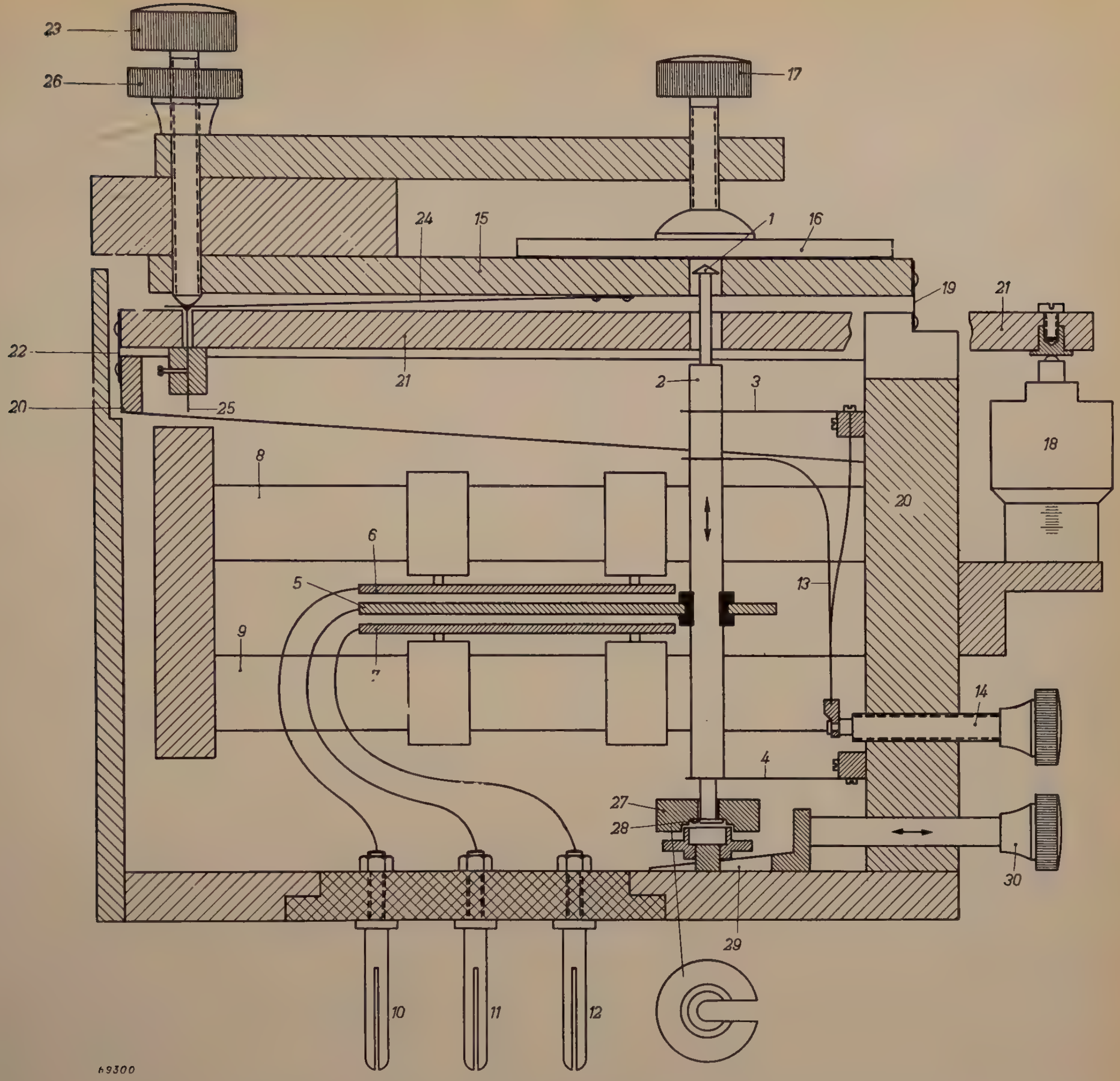

Fig. 3. Vertical cross section of the indentation meter (not to exact scale). The ram *2* with the sapphire *1* is supported by flat springs *3* and *4*; *5* is the movable plate of a differential capacitor, *6* and *7* being the fixed plates, supported by porcelain rods *8* and *9*. Plug pins *10*, *11* and *12* are for connection to the "Philoscope" bridge; *13* is a steel wire spring controlled by screw *14*. The specimen, *16*, is fixed to the platform *15* by means of screw *17*; *18* is the micrometer screw which, in conjunction with the beam *21* and adjustable screw *23*, controls and indicates the height of the platform *15*; *19*, *22* and *24* are flat springs. Spring *24* is attached to beam *21* by a short piece of steel wire *25*; *26* is a lock nut and *27* a slotted ring-shaped weight of 10, 5, $2^1/_2$ or 1 g. This weight rests on a shoulder *38* of the ram *2* and is lifted by a wedge *29* which is operated by means of knob *30*. When this knob is pressed, and the weight lifted, springs *3*, *4* and *13* can force the ram and sapphire upwards.

level with the tip of the sapphire, the micrometer screw *18* being set to a fairly high position. Once this preliminary adjustment has been effected, screw *23* is locked by means of the lock nut *26*. No re-adjustment is then neccesary unless the sapphire is replaced.

A flat spring *24*, situated between screw *23* and the platform *15*, is attached at one end to the platform, the other end being fastened to the beam *21* by the steel wire *25*. This ensures that any movement of the platform with respect to the beam will be free from play and also that the point of the screw *23* does not come in direct contact with the beam (friction between the point of the screw and the beam would cause the platform to move sideways when the screw is turned).

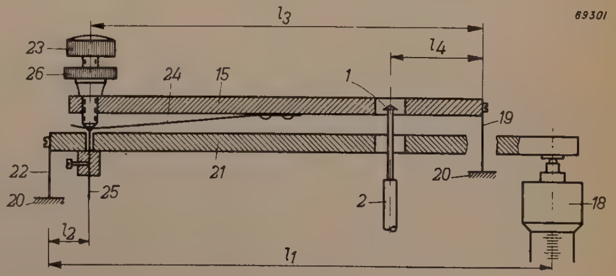

Fig. 4. Transmission of vertical displacement of micrometer screw *18* to platform *15* with a reduction of 50:1 (with respect to the sapphire *1*). Numbers correspond to those in fig. 3. l_1, l_2, l_3 and l_4 are lever dimensions.

The scale on the micrometer screw gives a reading which is accurate to within $\frac{1}{2}$ scale division, or 0.05 μ.

When the specimen is clamped to the platform and the bridge is balanced with the sapphire not yet touching the paint, the next step is to lower the specimen until the paint just touches the sapphire (as in fig. 1*b*-*c*). This is done by adjusting the micrometer screw, thereby lowering the platform. Contact can be said to be established at the first signs of unbalance of the bridge: sensitivity of the instrument is such that a load of only 3 mg on the sapphire is sufficient to give a visible deflection of the electronic indicator. A load equal to twice this value gives a pronounced indication. The initial load applied to the paint by the sapphire is therefore small compared with the load of 1 to 10 g with which the indentation is effected. Moreover, the initial load is applied only momentarily.

Fig. 3 shows the mechanism through which the initial load is applied. The ram *2* which carries the sapphire and is forced upwards by the flat springs *3* and *4* and, eventually by the steel wire spring *13*, has a ring *27* of which the weight is, say, exactly 10 g. When the knob *30* is pressed, wedge *29* lifts this ring, thus taking its weight off the shoulder of the ram. Instead of the force exerted by this weight of 10 g, an equivalent reactive force is exerted by the film of paint to the sapphire. If the resultant impression in the paint is too deep, the ring weighing 10 g may be replaced by one weighing 5, $2\frac{1}{2}$ or 1 g. At present, all measurements are carried out with a weight of 2.5 g. The indentation is then still small enough to be independent of the thickness of the coat of paint, but sufficiently large to be measured with sufficient accuracy.

As the rings are slotted to fit the ram, they are easily changed. In that case the position of the capacitor plate *5* must be readjusted by means of set-screw *14*.

If the specimen were left in the same position after the sapphire has penetrate the surface of the paint, the deflection of the flat springs (*3* and *4* in fig. 3) would decrease, i.e. they would lose some of their tension, with a corresponding reduction in the force exerted by them. It is desirable, however, to maintain a constant load for 30 seconds, and, accordingly, as soon as the weight *27* is lifted, the platform supporting the specimen is lowered slightly by means of the micrometer screw *18*, the adjustment being continued for 30 seconds so that the bridge remains balanced, i.e. that the spring tension remains constant.

As already mentioned, the minimum force with which the sapphire first comes in contact with the paint is 3 mg. This low pressure is ensured by using very flexible material for the flat springs *3* and *4*. The initial load of 3 mg corresponds (before contact is established) to a displacement of 0.03 μ of the movable plate of the capacitor, this being the minimum displacement to which the electronic indicator will respond when the bridge is balanced. In spite of this high sensitivity, no special steps need normally be taken to protect the instrument from vibration, this being probably due to the damping effect of the air in the confined spaces between the capacitor plates.

The over-all accuracy of the instrument is, however, determined not by the electrical but by the mechanical part of the instrument, i.e. the accuracy with which the adjustment of the micrometer screw can be reproduced, in this case to within 0.1 μ. This very slight amount of play is probably attributable not to the suspension springs, but to the thread on the screw and the point of contact between the screw and the beam.

By using an aluminium alloy for the framework and some of the components, a light but strong construction is secured; owing also to its small dimensions, the unit is easily transportable. Vulnerable components such as the differential capacitor are so housed as to be inaccessible unless the instrument is opened, and they are thus protected against damage and dust under normal working conditions.

The use of the instrument does not require much routine.

Results of some measurements

Measured values of the penetration depth *i*, taken from some of the most common types of paint, are given in the following *table* for the guidance of the reader. The loads applied by the sapphire were 2.5 g and 10 g. Notwithstanding the objections to the quantitative implication in the word "hardness" as applied to paints, the Vickers hardness *H* (= ratio of the load *F* to the area of the impression) is also specified in this table 6), merely

---

6) The lateral area A of a square-based pyramid with height i and apex angle φ is

$$A = i^2 \cdot \frac{4 \tan \frac{1}{2}\varphi}{\cos \frac{1}{2}\varphi} .$$

For $\varphi = 136°$, this is

$$A = 26.4\ i^2 .$$

Therefore, the Vickers hardness $H = F/A$ is

$$H = \frac{38\,F}{i^2}\ \text{kg/mm}^2,$$

with F in grammes and i in microns.

to give an impression of the order of magnitude.

For comparison it should be noted that the Vickers hardness of a diamond is 2600, that of a sapphire 1850, of hardened steel 200-950, of non-hardened steel 100-200, of copper 60, of lead and tin 5, all values being in kg/mm².

Penetration depths $i_{2.5}$ and i_{10} and Vickers hardness H of a few types of paint, with a load of 2.5 g, respectively 10 g, applied for 30 seconds at 20 °C.

Type of paint	$i_{2.5}$ µ	i_{10} µ	H kg/mm
Artists' paint	≫20	≫20	≪1
Decorators' paint	>20	>20	<1
Enamel for lighting fittings etc.	4.5-3	9-6	5-10
Synthetic paint for automobiles (synthetic resin, without nitro-cellulose) .	6-3.5	14-7	2- 8
Nitro-synthetic paint for automobiles	5-3	10-6	4-10
Lacquer for radio cabinets	4-3	7-5.5	8-12
Cycle enamel (stoved) . .	3-2.5	6-4.5	10-20

Only those types of paint of which the H-value is under 5 kg/mm² are soft enough to be tested by scratching with the nail. According to the values in the table, many types of paint are too hard to be tested in this manner.

Influence of temperature

Generally speaking, the "hardness" of a paint depends highly on the temperature. In order to enable tests to be carried out at various temperatures, the specimen plate is heated by a flat, brass block having in it channels through which hot water from a thermostatically controlled boiler circulates.

This method was employed to test two types of paint at different temperatures (penetration load 10 g).

Temperature °C	White stoving enamel i_{10} in µ	White nitro-paint i_{10} in µ
20	5.6	6.8
30	7.6	9.4
40	9.5	13.8

This table shows that nitro-paint softens to a greater degree with increasing temperature than stoving enamel; the ratio of the i-value at 40° to that at 20° is 9.5 : 5.6 = 1.7 for enamel, and 13.8 : 6.8 = 2.0 for nitro-paint. This difference is explained by a comparison of the two types of paint: both consist of macro-molecules forming chains of various lengths, but, whereas the stoving enamel structure is strengthened by numerous "bridges" between the chains, no such bridges occur in the structure of the nitro-paint; hence the nitro-paint is more thermo-plastic than the enamel.

In view of the effect of the temperature, it is advisable to state at which temperature the hardness test is carried out whenever accuracy is at all important. It is further recommended that, whenever possible, measurements be effected at not too low a temperature, e.g. 20 ± 0.5 °C, or that the values measured be referred to this temperature by interpolation or extrapolation.

Effect of layer thickness

The question of the layer thickness is an interesting one. Depicted in *fig. 5* are curves representing i as a function of the thickness d of a layer of a relatively soft, nitro-synthetic paint, each curve being plotted with respect to a constant load F, at a temperature of 25 °C. The thicknesses tested were 190, 120, 50, 20 and 10 µ, and in each case the specimen was thoroughly dried before the test. It appears that similar loads produce deeper impressions according as the thickness of the layer is increased 7), but that, at thicknesses above a certain limit — the greater the load F, the higher this limit —

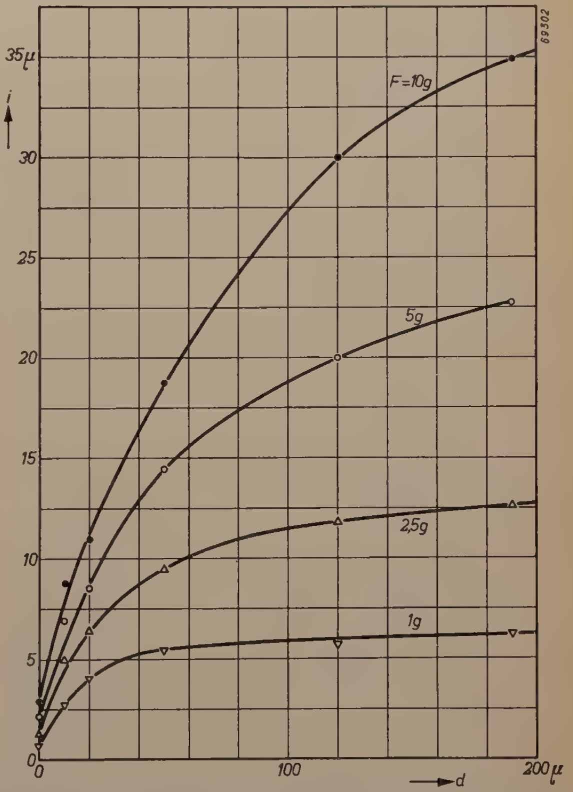

Fig. 5. Penetration depth i as a function of the thickness d of a coat of a relatively soft nitro-synthetic paint, for various values of the load F applied at 25 °C.

---

7) This effect is important not only from the point of view of testing, but also in its application: a thin coat of paint is apparently more resistant to mechanical damage than a thick one, or, for the same resistance to damage, the thin coat may be more plastic. Moreover, a thin film is more economical and is better able to follow deformations of the underlying surface.

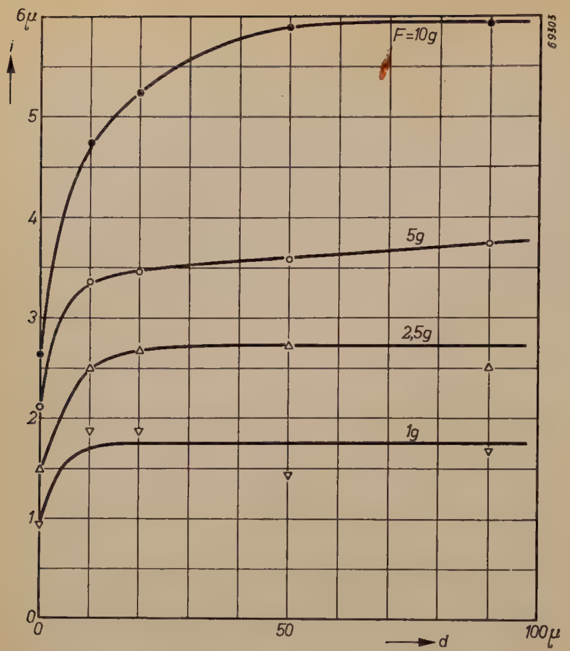

Fig. 6. As fig. 5, but for a slightly harder paint.

any further increase in d produces only a slight increase in i. Numerous tests have proved that, if a measurement is to be taken in the range in which i is only slightly dependent on d, the load F should be so small that i does not exceed one-twelfth of d.

Curves relating to a slightly harder paint and also to a hard stoving enamel are shown in *figs* 6 and 7.

The curves connecting the measured points in figs. 5, 6 and 7 seem by interpolation with respect to $d = 0$ to reach the i-axis at a point which, for the same value of F, gives the depth of penetration into the material to which the paint is applied.

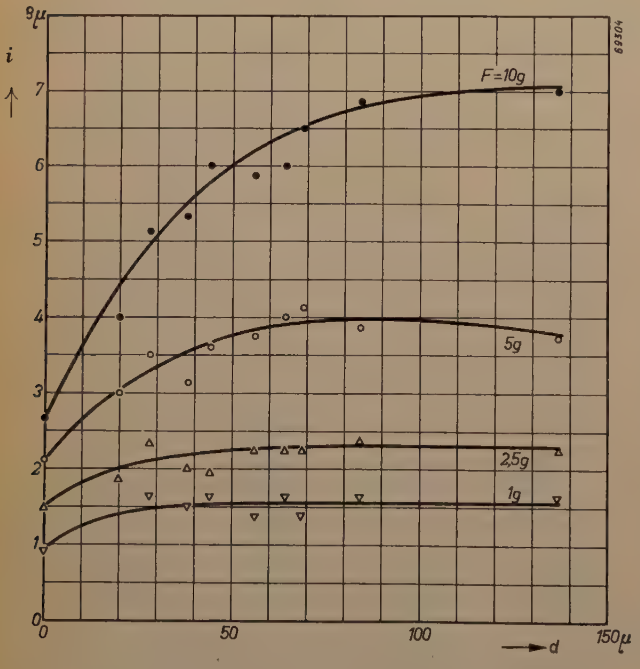

Fig. 7. As fig. 5, but for a hard stoving enamel.

In the tests conducted by the authors this material was aluminium with a hardness value of $H \approx$ 45 kg/mm^2. According as the thickness of the coat of paint decreases, the apparent Vickers hardness of the paint, based on the F-value and i-value, more and more approximates the H-value of the underlying material.

Figs. 5, 6 and 7 clearly show that, in the case of $d \to \infty$, the limit of the penetration depth increases more rapidly than $\sqrt{F}$; hence, with large thicknesses, the apparent hardness drops as F is increased.

Further test results are given in the original paper [8]).

Variation of the "hardness" during the drying process

The ultimate "hardness" in the thoroughly dry condition is not the only important property of a coat of paint: the period involved from the time of application until such time as the painted article can be safely handled is another important factor.

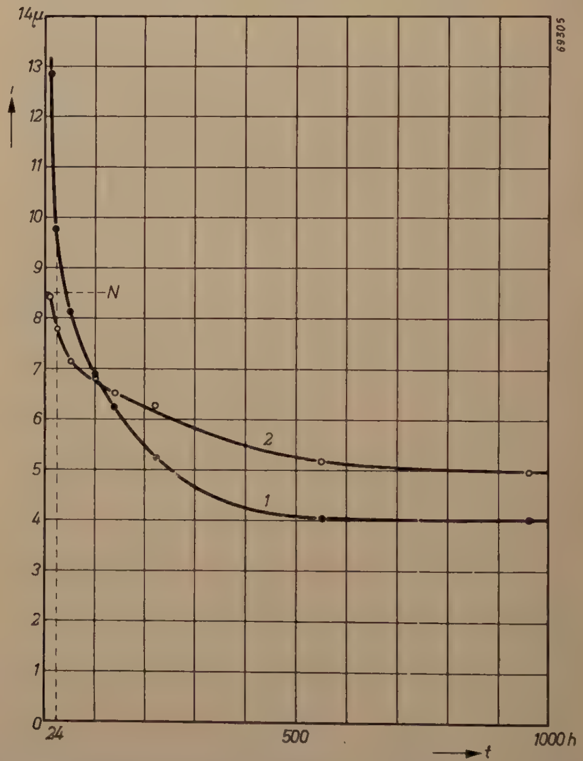

Fig. 8. Penetration depth i (with an applied load of 10 g) as a function of the drying time t, for two types of air-drying paint, both containing TiO$_2$ as pigment and identical volatiles. Type *2* reaches the value N (resistant to scratching) before type *1*.

The threshold of this condition may be said to be at the point at which the paint is "resistant to scratching" (penetration depth 8.5 μ at $F = 10$ g, or hardness value approx. 5 kg/sq. mm).

---

[8]) J. Hoekstra (also on behalf of J. A. W. van Laar), The purpose of measuring the hardness of paints (in Dutch), Verfkroniek 25, 13-17, 1952.

Fig. 8 shows the penetration depth as a function of the drying time of two types of physical drying paint containing identical volatiles and the same pigment (titanium dioxide), but differing slightly in composition (synthetic resin, plasticizer). When *i* no longer changes noticeably with time the paint in the deeper layers may also be entirely dry.

Curve *1* relates to a paint of a composition such that, although its ultimate hardness is fairly high (fairly low *i*-value), it reaches the state in which it is "resistant to scratching" much later than the paint represented by curve *2*, which, therefore, is to be preferred. Measurements of this kind are of very great value in the preparation of paints.

Summary. This article describes an instrument for the testing of painted surfaces, more or less along the lines of the Vickers hardness tester for metals. A sapphire of pyramidal form having an apex angle of 136° is pressed against the coating of paint with a force of 10 g or less. When pressure has been maintained for 30 seconds, the depth to which the sapphire has penetrated into the paint is measured by means of a differential capacitor which forms two branches of a bridge, the other two branches (resistors) being incorporated in a "Philoscope" bridge which also includes an amplifier, electronic indicator and power unit. Penetration depths of only a few microns can thus be measured with an accuracy within less than one-tenth of a micron. The instrument is robust, easily transportable and simple in operation.

A Vickers hardness could be deduced from the hardness measured, but this is inadvisable because the latter quantity depends to a large extent on the force with which the sapphire is pressed against the point.

Some examples are given to illustrate the effects of the temperature and the thickness of the coat of paint to be tested. When the thickness is below a certain limit, an "apparent" hardness, which is much higher than the true value, is measured; the penetration depth should therefore never be more than one-twelfth of the thickness of the coating if the effect of the layer thickness on the penetration depth is to be eliminated.

DIELECTRIC LOSSES IN GLASS

by J. M. STEVELS.

666.1:537.226.3

One of the many industries in which glass is used is that of electrical engineering. A problem arising in this industry is the behaviour of the glass in an electric alternating field. The dielectric losses of glass form one of the factors that decide this behaviour. Extensive investigations are still being carried out with a view to producing glasses having small dielectric losses at all frequencies. These investigations have not only led to an improvement of the existing kinds of glass but they have given a better insight into the physical and chemical structure of glass.

Dielectric losses

Glass is a material that is much used in electrical engineering: the bulbs of incandescent lamps and of radio valves (transmitting and receiving valves) are made from glass, that is also indispensable as an insulating material and for very many other purposes. It is therefore of great importance to know how the electrical properties of glass are affected by its composition, for this enables a choice to be made of the best kinds of glass for certain uses. This article will deal with the behaviour of glass in an electric alternating field, attention being mainly focused on the dielectric losses of glass.

When a piece of glass is interposed as a dielectric between the plates of a capacitor and an alternating voltage with a frequency f is applied to that capacitor, if the glass were free of losses, then the current flowing through the circuit would be exactly an angle $\pi/2$ in advance of the voltage across the capacitor. This means that no energy would be dissipated in the capacitor. In practice, however, every dielectric, and thus also glass, dissipates a smaller or larger proportion of the energy applied and converts it into heat. The measure of this dissipation of energy (the dielectric losses) is denoted by the angle δ by which the actual difference in phase between current and voltage deviates from $\pi/2$. The energy dissipation per unit of time for a small δ is approximately equal to $f \tan\delta$; the angle δ is called the loss angle.

In glass, as is the case with other materials, the dielectric losses vary strongly with the frequency of the electric field. The "spectrum" of the losses of glass is broadly represented by the fully drawn curves in *fig. 1*, which have been drawn for two temperatures, viz. 50 °K and room temperature. It is to be noted, however, that these diagrams have no quantitative significance; the losses differ greatly according to the kind of glass considered. The graph gives only a general impression of the losses as a function of frequency. Although the frequency range in these diagrams extends from 1 to 10^{14} c/s, only measurements between the frequencies of 50 c/s and 10^{10} c/s will be dealt with.

Fig. 1 reveals that there are two maxima of the losses, shifting in frequency as the temperature is changed but not in the same direction. Between the maxima is a "valley" of relatively small losses, the depth of this valley decreasing as the temperature drops.

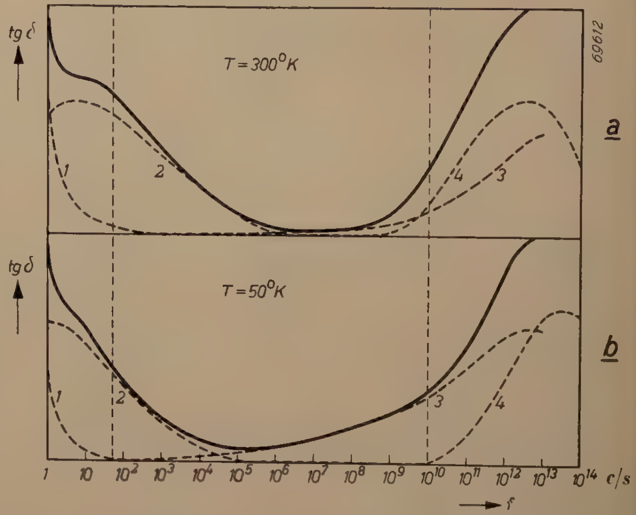

Fig. 1. Diagrammatic representation of the frequency spectrum of the dielectric losses in glass; *a* gives the spectrum at approximately room temperature, *b* shows how the spectrum appears at a very low temperature. The fully-drawn curve gives the total losses. It can be analyzed into four kinds of losses occurring at different frequencies, as represented by the broken-line curves: *1* conduction losses, *2* relaxation losses, *3* deformation losses, *4* vibration losses. It is seen how the vibration losses, occurring at high frequencies, are displaced to still higher frequencies as the temperature falls. The conduction and relaxation losses, on the other hand, are displaced towards lower frequencies, while the deformation losses increase over the whole line. These diagrams are of only theoretical significance. The frequency range here extends from 1 to 10^{14} c/s; this article deals only with the range between 50 and 10^{10} c/s (vertical broken lines).

From what is already known about the behaviour of the dielectric losses in other solids an attempt may be made to analyze the loss spectrum of glass into various components, taking into account the specific property distinguishing glass from crystalline materials, namely the relatively great disorder in the orientation of the ions from which glass is built up.

It will be seen that there are differences in the manner in which the various kinds of losses depend upon the composition of the glass. Thus from the analysis of the losses some idea can be obtained as to how the composition has to be varied in order to reduce or increase the losses at certain frequencies.

The result of the analysis has been graphically represented in fig. 1 by the broken-line curves. Four kinds of losses are to be distinguished, named respectively conduction losses, relaxation losses, deformation losses and vibration losses, which will now be dealt with in that order.

Conduction losses

Glass is not a perfect insulator. Under the influence of an electric force the network-modifying ions move through the whole of the network [1], and in doing so they give off part of the energy obtained from this force to the network in the form of heat.

The conduction losses (curve *1* in fig. 1) depend upon the conductivity σ according to the formula

$$\tan \delta = \frac{\sigma}{\omega \varepsilon' \varepsilon_0}, \quad \ldots \ldots \quad (1)$$

where ω $(= 2\pi f)$ represents the angular frequency of the electric alternating field and ε' the dielectric constant of the glass (ε_0 is the dielectric constant of vacuum). Thus $\tan \delta$ is inversely proportional to the frequency (since δ and ε' are not frequency dependent, or scarcely so), and the energy dissipation per time unit does not depend upon the frequency. This is a well-known property of a conductor. When $\tan \delta$ for a lime glass ($\sigma = 10^{-10}\ \Omega^{-1}\mathrm{m}^{-1}$, $\varepsilon' = 6$) is calculated according to the above formula for a frequency of 1000 c/s one finds the small value of 3×10^{-4}, whereas an actual measurement gives $\tan \delta = 100 \times 10^{-4}$, so that at this frequency there must be other causes of losses much more important than conduction. As a general rule, for frequencies higher than 50 c/s the conduction losses are negligible compared with the other losses. In this article, therefore, conduction losses will no longer be considered.

Relaxation losses

It is not only the transport of network modifiers through the whole piece of glass considered that causes losses, but also the transport over atomic distances in the glass plays a part. In *fig. 2* the variation of the potential energy of the ions in an arbitrary part of the network is indicated for an arbitrary direction (x) in that network.

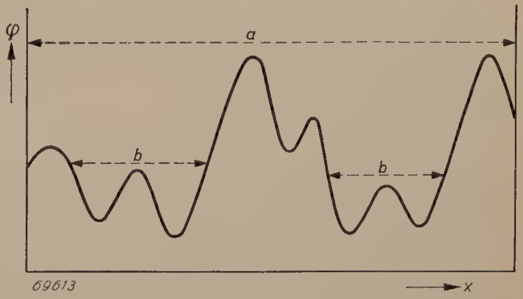

Fig. 2. The undulated curve represents the potential φ of the network-modifying ions along an arbitrary direction in the glass. The movement indicated by a can only be carried out by high-energy ions and corresponds to conduction, while the movement b is carried out by ions with less energy and results in relaxation losses.

The successive potential barriers, with varying heights and distances, form obstacles preventing an ion from travelling further through the glass. The potential barriers arise partly from electrical causes (mutual repulsion of the ions) and partly from purely geometrical causes: the movement of the ion concerned may be obstructed by the other ions. Similar potential barriers are found also in crystals, but there the distances and heights are very regularly distributed.

When an electric field is applied the ions tend to move in the direction of this field. Usually the field alone will not be sufficient to carry the ions over the potential barriers. For that to take place the ions have to take up extra energy, and this is obtained from collisions with other ions due to the thermal movement in the glass. It takes some time, however, before the ions have accumulated sufficient energy to pass over a potential barrier; this time is called the relaxation time τ. If the electric field is an alternating field with angular frequency ω, and ω is not large compared with $1/\tau$, then during each half cycle the ions will have ample time to jump over one or more potential barriers, thereby gaining energy from the field, which is transmitted to the network in the form of heat; one then speaks of losses. At very low frequencies ($\omega \ll 1/\tau$) these losses are small, because then the ions already jump when the instantaneous value of the field differs but little from zero: the energy gain of the ions is then small and the lattice receives little energy.

---

[1] The structure of glass, and especially the conceptions of network-modifying ions and network-forming ions, have been dealt with in a previous article recently published in this journal (J. M. Stevels, Philips Techn. Rev. **13**, 293-300, 1952, No. 9), which will further be referred to as article I.

When, however, ω becomes of the order of $1/\tau$ then, on the average, the ions will not pass over the potential barrier until the field has practically reached the maximum value. The ions then gain much energy and the losses are large. If the frequency of the alternating field is much higher than $1/\tau$ the ions jump independently of the phase of the alternatng field and the losses are again small.

The relation between these relaxation losses and the angular frequency ω of the field is expressed as

$$\tan\delta = \frac{\omega\tau}{1+\omega^2\tau^2}, \quad \dots\dots \quad (2)$$

which is entirely in accordance with the foregoing reasoning: the losses occur only at angular frequencies round about $1/\tau$.

As may be understood from fig. 2, in glass there is more than one relaxation time τ, since the local structures differ considerably. This makes the relaxation losses perceptible over a relatively rather wide range of frequencies. The spectrum of these relaxation losses (broken-line curve *2* in fig. 1) shows a wide peak, the limits of the range in which the losses occur lying, at room temperature, at about 10^{-3} and 10^6 c/s. As already remarked, at frequencies higher than 50 c/s the relaxation losses exceed the conduction losses considerably.

The conduction losses could also be regarded as a kind of relaxation losses. The ions which collect sufficient energy to pass over the highest potential barriers will be able to travel through the whole piece of glass. In order to pass over the highest barriers, a very long relaxation time will obviously be required, and in that case formula (2) becomes

$$\tan\delta \sim \frac{1}{\omega\tau}, \quad \dots\dots\dots\dots \quad (3)$$

$\tan\delta$ being inversely proportional to the frequency, a relation applying, indeed, for conduction losses.

Deformation losses

Relaxation losses are therefore due to an after-effect phenomenon. There is reason to assume that another kind of losses occur in glass which bear the character of after-effect losses. These are denoted by the name of deformation losses to distinguish them from the relaxation losses just dealt with. Deformation losses do not arise from the movement of individual network modifiers, but from the movement of whole sections of the network, in particular a sort of kinking movement of the chains of the network (see I). As is rather obvious, such a phenomenon has a very short relaxation time: it is to be imagined that the chains make movements resembling the jumping of a bent leaf spring. Here again there are a large number of different relaxation times τ. Since on the average τ is very small, for the range of not too high frequencies formula (2) may be written approximately (for the case where there would be only one relaxation time) as:

$$\tan\delta \sim \omega\tau \quad \dots\dots\dots \quad (4)$$

From this formula it follows that the deformation losses increase about proportionately with the frequency and in most cases will be very small. The spectrum of the deformation losses is represented in fig. 1 by the broken-line curve *3*.

Vibration losses

The fourth kind of dielectric losses to be expected in glass are due to a resonance phenomenon. The ions in the glass — both the network formers and the network modifiers, as well as the oxygen ions — may vibrate with a certain frequency round about their state of equilibrium, and this they will in fact do as a consequence of the thermal movement. Regarding the ion as a harmonic oscillator, its frequency of vibration may be approximately represented by the formula

$$\omega_{\mathrm{res}} = \sqrt{\frac{a}{M}}, \quad \dots\dots\dots \quad (5)$$

where a is the proportionality factor denoting the relation between the restoring force and the displacement from the state of equilibrium, and M is the mass of the ion in question. Consequently ions of different mass and ions at different places in the crystal (with different a) will usually vibrate with different frequencies.

When an electric force is applied with a frequency approximately equal to the vibration frequency of an ion, then resonance may occur. Since the vibrations of the ions are always damped, this resonance is accompanied by losses. If all the ions had the same resonant frequency, then the spectrum of these vibration losses would show a maximum round about that frequency. But, as already observed, there are a large number of resonance frequencies. This, and the possibility of the vibrations of the ions being strongly damped, leads to a wide maximum in the spectrum of the vibration losses. This spectrum is represented in fig. 1 by the broken-line curve *4*. Unfortunately, with one single exception, the actual maximum has never yet been determined, since measurements so far carried out have not gone beyond 10^{10} c/s.

Vibration losses in glass are directly comparable to the well-known infra-red absorption in polar crystals, which arises from a similar resonance phenomenon. In the case of a crystal like rock salt this absorption takes place at about 10^{13} to 10^{14} c/s, where the maximum is very narrow. The fact that in the case of glass "spurs" of the vibration losses are to be observed at much lower frequencies (about 10^{10} c/s) may be ascribed, as already explained above, on the one hand to the presence of ions with low resonance frequencies and on the other hand to the possibility of a strong damping of the ion vibrations in glass, which leads to a considerable widening of the loss spectrum. As may be understood theoretically, strongly damped resonance vibrations form, as it were, a transition to the relaxation vibrations previously discussed. The question in how far the vibration losses in glass are to be regarded purely as a resonance phenomenon or as a sort of after-effect phenomenon can to a certain extent be answered, as will presently be shown, when the temperature dependency of the losses is investigated. It is to be added, however, that in order to gain a deeper insight into these phenomena it is necessary to study the losses in glass in the infra-red at the frequencies of 10^{11} to 10^{13} c/s unfortunately it is extremely difficult to carry out absorption measurements in that range.

Having now dissected the total loss spectrum in fig. 1 into four components, the spectrum can be well understood qualitatively. For a quantitative investigation great difficulties have to be overcome, due to the irregular structure of glass. Some confirmation of the picture formed is, however, to be obtained when we come to investigate the temperature dependency of the various kinds of losses. It is then found that their behaviour is roughly as represented in figs 1*a* and *b*, the relaxation and conduction losses being displaced towards lower frequencies as the temperature drops, while the deformation losses increase over the whole line. As to the vibration losses, there are indications that with falling temperature these are displaced towards higher frequencies, and this would be in agreement with what is to be theoretically expected for this kind of loss.

Influence of temperature upon the losses

The foregoing conclusions may be briefly explained as follows.

The temperature dependency of conduction losses is governed entirely by that of the conductivity. As is presumably known, for a fixed frequency the conductivity σ decreases with falling temperature, and thus, according to formula (1), also the conduction losses decrease.

The relaxation times τ occurring with relaxation losses and deformation losses will be greater as the temperature T falls, since the mutual collisions of the ions are then fewer and weaker and it takes longer for the ions to accumulate the energy required to overcome a potential barrier. An increase in τ means a displacement of the losses to lower frequencies, as is indeed observed in the case of relaxation losses when T drops.

As to the deformation losses described by formula (4), an increase in τ means that the losses increase over the whole of the frequency range with which we are concerned. For a quantitative calculation of the temperature dependency of relaxation and deformation losses it is necessary to take into account the great variety of relaxation times occurring in glass, but in their generality the conclusions still hold. To illustrate the relation between the losses at medium frequencies and the temperature, in *fig. 3* a curve has been plotted representing tan δ of a lime glass as a function of temperature at the frequency 1.5 × 10^6 c/s. It appears that, for temperatures round about 70 °K, tan δ shows a broad maximum, then becoming rather small at about 150 °K and rising again rapidly at temperatures higher than 200 °K. The broad maximum is due to the deformation losses, while the rise above 200 °K is to be ascribed to relaxation losses, as may be understood from the following.

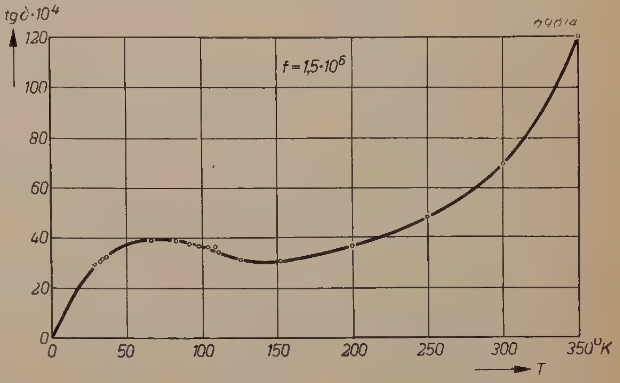

Fig. 3. Dielectric losses in a lime glass at the frequency 1.5 × 10^6 c/s as a function of temperature. The maximum at low temperatures corresponds to the deformation losses, the rise of the curve on the right is due to relaxation losses.

For a fixed frequency it is possible to determine the temperature at which the deformation losses have reached their maximum. The relaxation times are always much smaller for the deformation losses than for the relaxation losses, so that the frequency mentioned will be situated on the right-hand descending part of the frequency curve for the relaxation losses. When the temperature rises both the spectrum of the deformation losses and that of the relaxation losses will be displaced towards higher frequencies. The maximum of the deformation losses will, therefore, move away from the fixed frequency, whereas the maximum of the relaxation losses moves towards this frequency.

A note is to be added here. The conduction loss is also a kind of relaxation loss, with such a great relaxation time as to occur always on the right-hand descending part of the curve representing the relation between losses and frequency. The conclusion already arrived at in another way, that these conduction losses diminish with falling temperature, is therefore not surprising when considered also from this point of view.

Purely vibrational losses will be displaced towards higher frequencies as the temperature falls. This is because the vibrating ions have on the average higher resonant frequencies at lower temperatures, as may be understood from quantum theory. It has already been pointed out that the vibration losses in glass probably form a transition to relaxation losses. Since the temperature dependency of relaxation losses is just the reverse of that for vibration losses, it is not possible to predict the influence of temperature on these losses at the highest frequencies without carrying out further experiments in the far infra-red. The indication, already mentioned, that with falling temperature these losses are displaced to higher frequencies makes it highly probable, however, that the character they bear is preponderantly that of resonance.

We now have to consider the influence of the composition of the glass upon the different kinds of losses. First its influence upon the relaxation losses will be dealt with, and then the influence upon the vibration losses; as mentioned above, the conduction losses will be disregarded, since, whatever the composition of the glass may be, for frequencies above 50 c/s they are of no importance; as to the deformation losses too little is yet known about them.

Influence of the chemical composition of glass upon relaxation losses

The manner in which relaxation losses are affected will be considered under five headings.

Nature of the ions

As a rule only those network modifiers which readily migrate through the glass will be capable of yielding a considerable component towards the relaxation losses. The mobility of the ions in a given potential field is determined mainly by their size: it is particularly the relatively small Li^+ and Na^+ ions which play an important part in this respect. Glasses containing a large proportion of these ions show high relaxation losses. The K^+ ion is so much larger that it contributes much less towards the losses. By way of illustration mention may be made of a series of low-melting glasses of the composition 53.3 mol % SiO_2, 10.2 mol % PbO, 4.5 mol % CaF_2 and 32 mol % M_2O, with M representing an alkali metal. For a frequency of 1.5×10^6 c/s and at a temperature of 20 °C, the value of tan δ for M = Li is 132×10^{-4}, for M = Na tan δ is 106×10^{-4} and for M = K it is 54×10^{-4}.

Divalent ions, owing to their larger charge, are bound more strongly to their surroundings and thus are usually less mobile. An exception is the small Mg^{2+} ion which appears to be capable of yielding a considerable contribution towards the losses.

From now on the Li^+, Na^+ and Mg^{2+} ions will be denoted by the name of mobile ions, whilst the divalent network modifiers, such as Ca^{2+}, Ba^{2+}, Pb^{2+}, will be called immobile ions.

It will be clear that the losses depend also largely on the nature of the network. This influence can be reduced to three effects.

Influence of R

As explained in article I, the ratio R of the number of oxygen ions to the number of network-forming ions is a measure for the coherence of the network from which the glass is built up. The larger the ratio R, the less coherent is the network and the less dense is the structure of the glass. This lends more mobility to the network modifiers, and the relaxation losses may be expected to increase.

Influence of the addition of immobile ions

If metal ions showing little mobility — either because they are large or because they are strongly bound electrically — are added to a glass of a certain composition, then there will be less possibility for displacement of the mobile ions. Thus, given equal concentration of mobile ions, the addition of immobile ions to a glass reduces its loss angle.

The effects mentioned here can be quantitatively described by the formula:

$$\tan \delta = A\, C_m\, R\, (1 - BC_i)\,, \quad . \quad . \quad . \quad (6)$$

where C_m represents the concentration of the

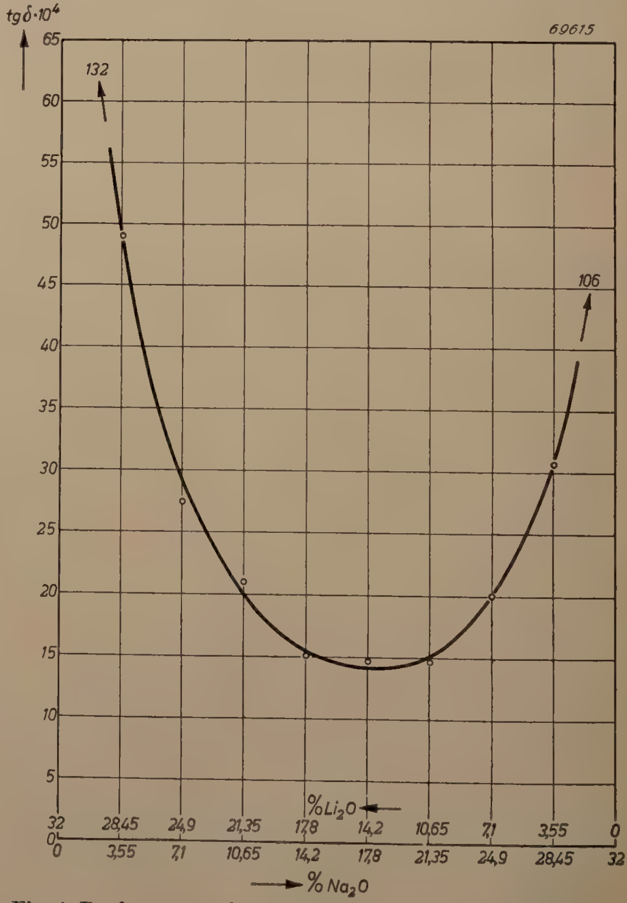

Fig. 4. Replacement of part of the Li+ ions in a lithium-silicate glass by Na+ ions gives a very rigid structure and thus reduces the relaxation losses. If, however, this replacement is carried too far the structure becomes less rigid again. The curve for tan δ therefore shows a minimum at about equal concentrations of Na^+ and Li^+ ions (measured at the frequency of 1.5×10^6 c/s).

mobile ions and C_i that of the immobile ones; the coefficient A depends on the frequency and temperature; B is a geometrical factor ²).

Difference in packing, with equal R

If in a glass containing only one kind of network modifiers, some of these ions are replaced by other network modifiers having a different radius, then a more compact network can be obtained. As the glass cools from the melt, the mutually coherent chains of network-forming ions will then preferentially so arrange themselves that the largest interstices in the network are occupied by large network modifiers and the smallest interstices by small network modifiers. The resulting denser structure leads to a reduction of the losses. This is illustrated in *fig. 4*, relating to the glass of the composition mentioned in the beginning of this section, with M representing partly lithium and partly sodium. The value of tan δ (measured for a frequency of 1.5×10^6 c/s) varies with the variation of the proportions of Na^+ and Li^+; the losses are the smallest with about equal molecular concentrations of Na^+ ions and Li^+ ions.

Relaxation losses in borate glasses

In article I it has already been discussed how in certain respects the structure of borate glasses differs from that of other glasses. In a glass of the composition x Na_2O-y B_2O_3, if $x < 18$ mol % (the

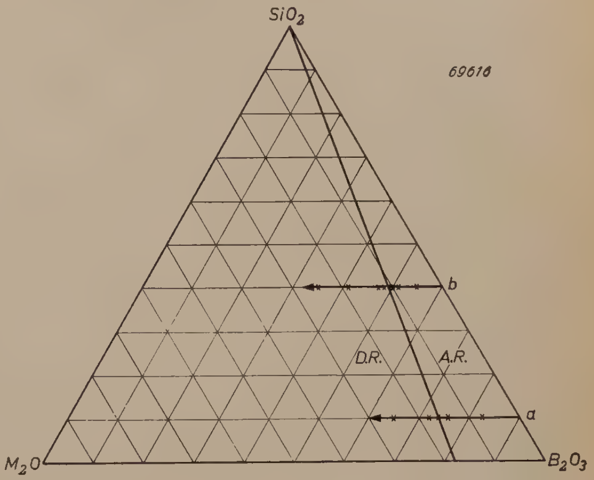

Fig. 5. Phase diagram of the ternary system M_2O-B_2O_3-SiO_2, the borosilicate glasses. M represents an alkali metal. Two regions can be distinguished: the accumulation region *A.R.* and the destruction region *D.R.*

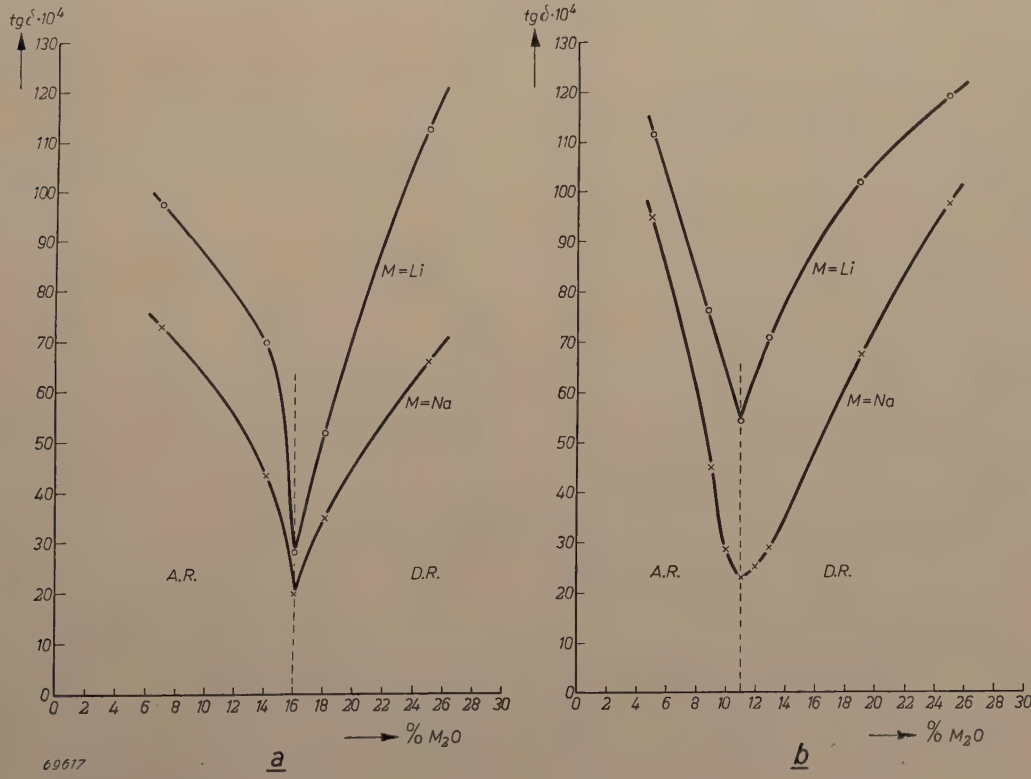

Fig. 6. Variation of tan δ with the Na_2O or Li_2O content of borocilicate glasses; *a*) corresponds to the compositions *a* in fig. 5, *b*) corresponds to the compositions *b*. The curve for tan δ shows a sharp minimum on the *A.R.-D.R.* separating line. It is also seen that Li ions cause a larger loss angle than Na-ions, because the former are more mobile. Measurements were taken at the frequency of 1.5×10^6 c/s.

---

²) See, e.g., J. M. Stevels, Progress in the theory of the physical properties of glass, Elsevier Publ. Co., Amsterdam 1948, p. 76.

accumulation region), the network-modifying Na^+ ions are incorporated in the network without any breaking of oxygen bridges, and thus there are no non-bridging oxygen ions. This is due to the fact that the B^{3+} ions may occur both in the centre of an oxygen triangle and in that of an oxygen tetrahedron. With larger concentrations of Na_2O, however, oxygen bridges tend to be broken, and this range of concentrations is called the destruction region.

With increasing concentration of Na_2O in the accumulation region, the network becomes more and more rigid until the maximum rigidity is reached just at the transition concentration of 18 mol % Na_2O, above which it begins to loose its rigidity again. Such has been illustrated in article I with reference to the behaviour of the expansion coefficient of the glass as a function of its composition.

A similar phenomenon arises in the case of borosilicate glasses. In *fig. 5* a phase diagram is given for the system M_2O-B_2O_3-SiO_2, where M stands for a monovalent network modifier. This diagram can be divided into an accumulation region *A.R.* and a destruction region *D.R.* The compositions found along the line separating these two regions are characterized by a maximum rigidity of the structure.

Obviously the dielectric losses (conduction and relaxation losses) will be influenced by this change in structure. As was to be expected, the losses show a decided minimum just on the dividing line, as is illustrated in *fig. 6*. Fig. 6*a* corresponds to the compositions indicated by the arrow points *a* in fig. 5. Fig. 6*b* applies for the compositions *b* in fig. 5. Both Li^+ and Na^+ have been chosen as monovalent network-modifying ions, thus giving two perfectly analogous curves.

Influence of the chemical composition of the glass upon the vibration losses

It is possible to shift the frequency range of the vibration losses by changing the composition of the glass. The influence of the chemical composition will again be considered from a number of points of view.

Nature of the ions

One of the most important factors affecting the frequency of the vibration losses is the mass of the ion (cf. formula (5)). The heaviest ions will give the lowest resonant frequency; thus the addition of heavy ions causes the vibration losses to be displaced to lower frequencies. The charge of the ions plays a less important part (this occurs in the restoring force constant *a*, which expresses the interaction of the ion with the surroundings).

Influence of R

The larger the ratio *R*, the less dense is the network. The ions become more loosely bound to their surroundings and the resonant frequencies are shifted to lower frequencies. Phosphate glasses are of a kind in which many non-bridging oxygen ions occur and thus the ratio *R* is high. *Fig. 7* shows that in a certain phosphate glass the resonant frequencies are shifted so far that the maximum of the

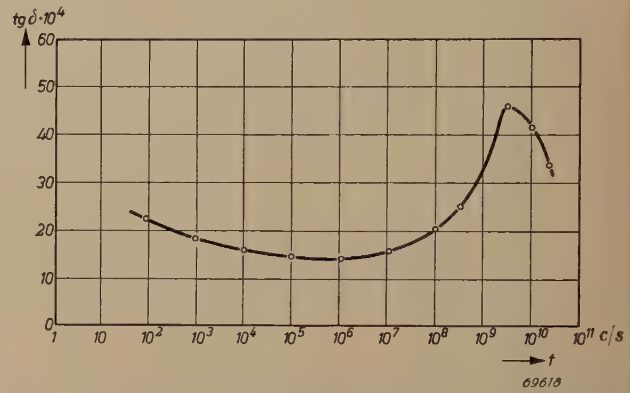

Fig. 7. Example of a glass (phosphate glass) in which the resonant frequencies lie very low, within the frequency range accessible for measurements.

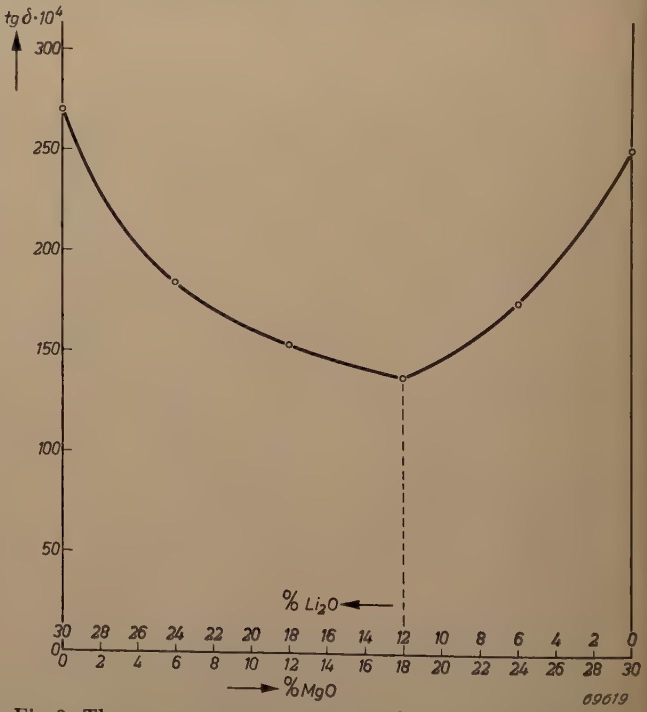

Fig 8. The more compact structure of a silicate glass due to the presence of different kinds of network modifiers leads to a reduction of the vibration losses, measured at a frequency of 2.4 × 10^{10} c/s. This diagram is fully comparable with fig. 4. It is to be noted that the value of *R* in this diagram, going to the right, drops somewhat, the reason for this being that Mg^{2+} ions, if present in large concentrations, have the tendency to act as network formers. This diagram relates to a glass of the composition 70% SiO_2 and 30% (Li_2O+ MgO).

vibration losses is situated below 10^{10} c/s (this is so far the only case where it has been possible to measure such a maximum).

The addition of some metal oxides, such as Al_2O_3 and ZnO, which reduce *R*, will lower the losses at higher frequencies, as follows from the foregoing.

Difference in packing, with equal R

As already seen when discussing the relaxation losses, the structure of the network becomes more compact the more the network-modifying ions occurring in the glass differ from each other in their dimensions, even when *R* remains constant. The more compact the network, the higher are the resonant frequencies of the vibration losses and thus the less are these losses noticed in the range of the relatively low frequencies where the measurements are taken. An illustration of this is given in *fig. 8*, which is directly comparable with fig. 4.

Vibration losses in borate glasses

The effect of the transition from *A.R.* to *D.R.* upon the vibration losses is exactly comparable to the effect upon the relaxation losses. In the neighbourhood of the transition the network is very rigid, and thus the resonant frequencies are very high. The "spur" of the vibration zone that can be measured is then small. This is illustrated in *fig. 9*.

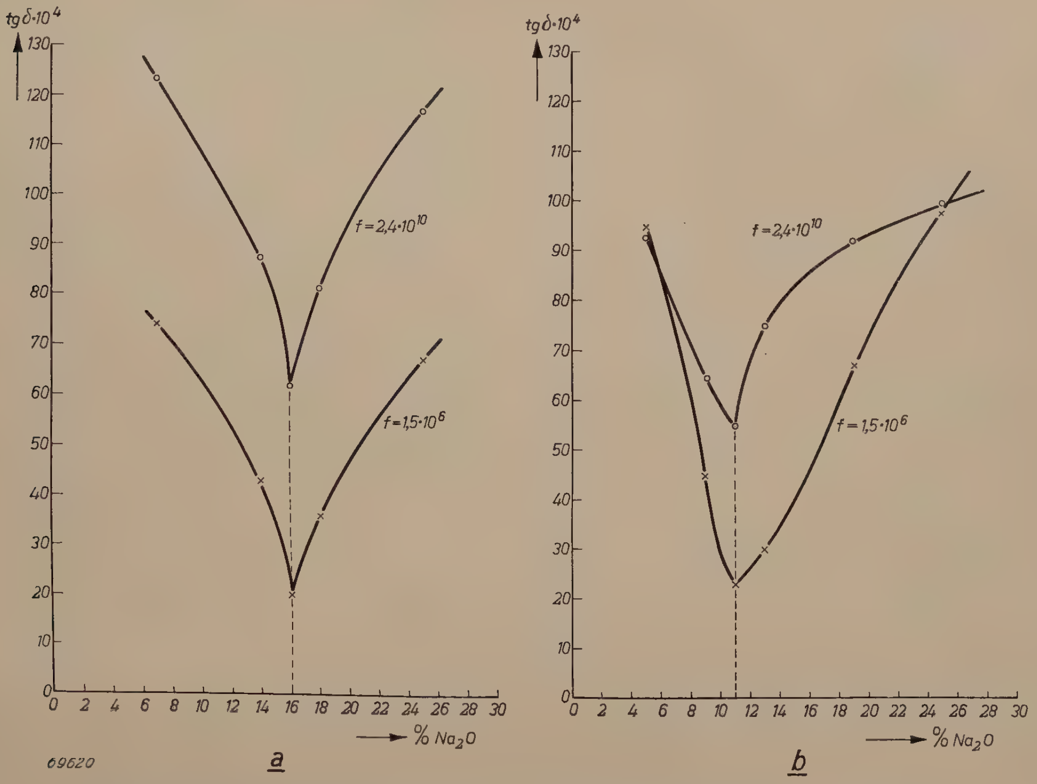

Fig. 9. The vibration losses in borate glass, just as the relaxation losses, are affected by changes in composition going from the *A.R.* to *D.R.* region. Fig. 9*a* relates to the compositions *a* in fig. 5, fig. 9*b* to the compositions *b*, with Na^+ as network modifier. The vibration losses have been measured at 2.4 × 10^{10} c/s; for comparison also the relaxation losses measured at 1.5 × 10^6 c/s are reproduced from fig. 6.

Some examples of the spectrum of dielectric losses in glass

Fig. 10 gives the tan δ as a function of frequency for a number of glasses. The region of the relaxation (and conduction) losses on the left and that of the "spurs" of the vibration losses on the right are clearly distinguished. The glass *A* contains a large proportion of mobile ions and thus shows very large losses. The fact that the curve *D*, for lead glass, rises relatively more steeply at high frequencies than the other curves can be explained, according to the foregoing, by the presence of a large number of heavy ions, as a consequence of which the resonant frequencies lie lower than those in the other glasses.

Fig. 11 shows the losses of a lead-containing glass at a number of frequencies as a function of temperature. This is to be compared with fig. 3. The influence of the deformation loss at low temperatures is clearly seen. This influence is of

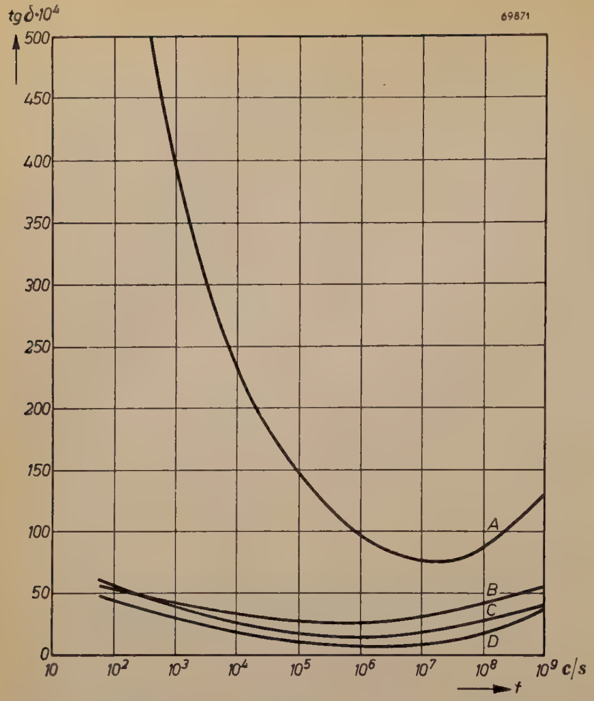

Fig. 10. Loss spectra of a number of glasses. *A* soda-lime glass; the losses, especially the relaxation losses on the left, are very high, owing to the large proportion of mobile Na$^+$ ions contained in the glass. *B* alkali-free silicate glass, and *C* borosilicate glass: these glasses have low losses. *D* lead glass: the losses for this glass show a relatively steep rise at higher frequencies, because the resonant frequencies in this glass are low.

particular importance for higher frequencies, as follows also from the theory. The increase in the losses at higher temperatures is again due to relaxation losses.

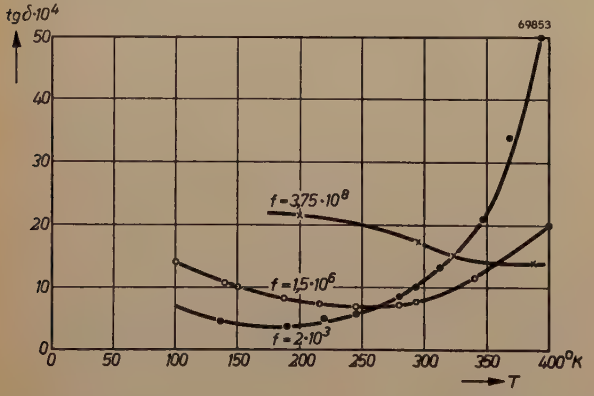

Fig. 11. Loss angle of the glass with the composition 45% SiO_2, 32% PbO, 5% CaF_2, 4% Na_2O and 14% K_2O, as a function of temperature, at different frequencies. The deformation losses (on the left of the diagram) are relatively considerable (cf. fig. 3), particularly at high frequencies.

Practical applications

Glasses with low dielectric losses

Although in practice glasses with high dielectric losses are sometimes desired for special purposes, these will not be discussed here. It has already been made sufficiently clear how such glasses can be produced.

Of most importance are the glasses which show small dielectric losses at normal working temperatures; these are used for the construction of all sorts of electronic tubes and valves. From the foregoing comments it follows that a distinction has to be made between (1) glasses intended for use at intermediate frequencies (radio valves), where the dielectric losses are mainly relaxation losses, and (2) glasses intended for constructions where very high frequencies are applied and mainly vibration losses occur. These are two entirely different fields; a glass that is satisfactory in one field need not at all be so in the other. It is certainly not difficult to find a glass with low dielectric losses at all frequencies — such as fused silica — but the difficulty lies in the fact that for these applications there are nearly always important secondary requirements to be met, e.g. that the glass should be easily workable, that its viscosity should not be influenced much by temperature, and so on. In electrical engineering the glass is required to have a certain expansion coefficient to allow of it being fused onto metals such as steel, chromium iron, fernico and tungsten.

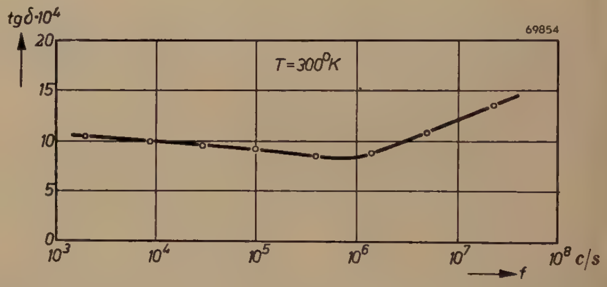

Fig. 12. Frequency spectrum at room temperature of the glass described under fig. 11. The great variety of network modifiers, including, i.a., also immobile Ca^{2+} and Pb^{2+} ions, causes the losses to be small and practically constant over a wide frequency range.

Most of the properties just mentioned can be obtained by using a high percentage of Na$^+$ ions in the glass, but then usually the losses are high. However, by making judicious use of the knowledge now acquired the losses can be appreciably reduced, while still retaining the other properties.

A good example is a glass of the composition 45% SiO_2, 32% PbO, 5% CaF_2, 4% Na_2O, 14% K_2O (weight percentages). Owing to its high contents of Na_2O, K_2O, CaF_2 and PbO, this glass softens at very low temperatures and has such a large expansion coefficient (120×10^{-7}) that it can be fused to iron, while at the same time it shows exceptionally small losses for the intermediate frequencies(see *fig. 12*; fig. 11 applies also for this glass). This is due to the addition of immobile ions

(Pb^{2+}, Ca^{2+}, K^{+}), while the presence of four kinds of network modifiers of different sizes promotes a good packing of the network. It is true that this glass has a relatively large R (viz. 2.64) — which gives it the low softening temperature — but this factor, which is unfavourable for the dielectric losses, is apparently sufficiently compensated by the other favourable factors mentioned above.

Investigation into the structure of glass with the aid of dielectric losses

Since small changes in the structure of glass often result in great changes in the dielectric losses, by applying the reverse process of reasoning it is often possible to draw interesting conclusions as to the structure of a glass from its dielectric losses.

A striking example of this is found in the dielectric properties of the borate glasses already discussed. The position of the separating line between the accumulation region and the destruction region (figs 5, 6 and 9), predicted on theoretical grounds, can be experimentally determined, i.a. from measurements of the dielectric losses.

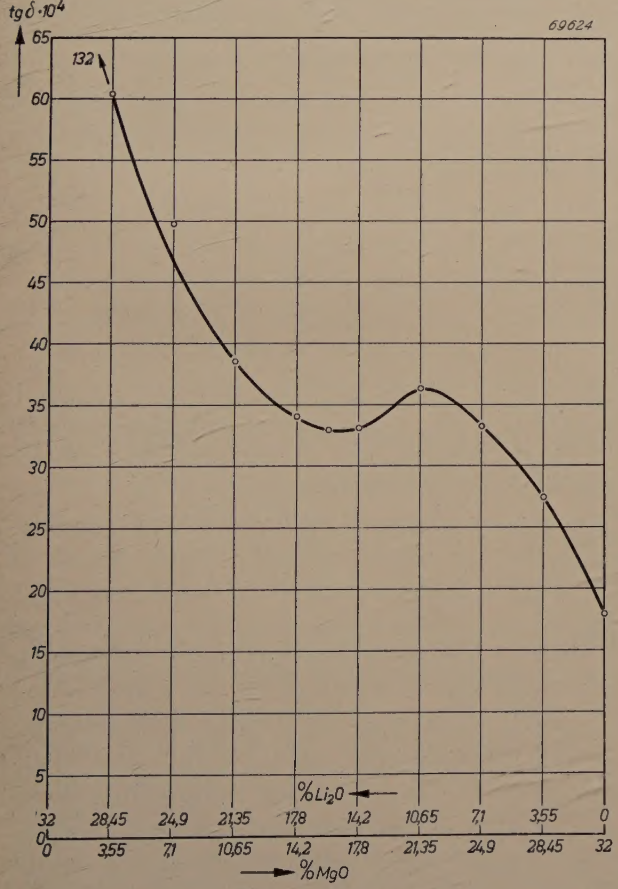

Fig. 13. Variation of tan δ at the frequency 1.5×10^6 c/s and at room temperature for a series of glasses of the composition 53.3% SiO_2, 10.2% PbO, 4.5% CaF_2 and 32% (Li_2O+MgO), as a function of the MgO percentage. As described under fig. 4, when some of the Li^{+}ions are replaced by Mg^{2+} ions, tan δ at first decreases, because the structure of the network is then more rigid. A further increase of the Mg^{2+} content reduces the rigidity of the structure and tan δ increases. This does not continue along the same line, in contrast to fig. 4, since the higher the Mg^{2+} concentration, the more Mg^{2+} ions begin to act as network formers. Then they no longer contribute to the relaxation losses, so that ultimately tan δ drops.

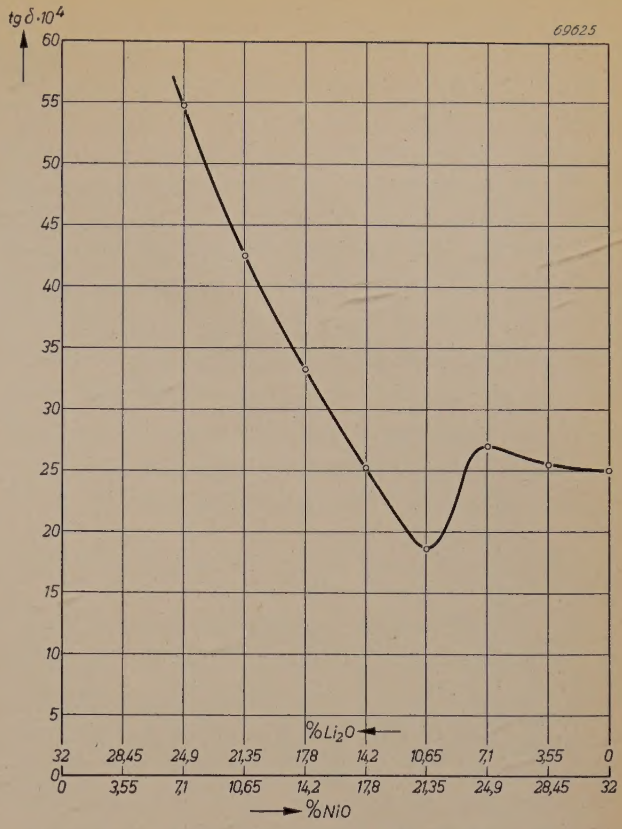

Fig. 14. This diagram relates to a glass analogous to that of fig. 13, but with the Li^{+} ions replaced by Ni^{2+} instead of Mg^{2+} ions. The curve has the same trend as that in fig. 13.

There is one other example that may be gone into more deeply. In article I it was stated that there are a number of cations which may occur both in a network-modifying and in a network-forming position. In a number of cases it is possible to see already from the colour of the glass how the ions behave. However, there are some ions (Mg^{2+}, Zn^{2+}) which do not colour the glass, and then the dielectric losses may serve as an indication how these ions are situated in the network. Particularly in the case of the Mg^{2+} ion most valuable information can thereby be obtained, for, as we have seen, this ion yields a rather considerable contribution towards the relaxation losses when occupying a network-modifying position, whereas it obviously contributes hardly anything at all to this kind of losses when it is in a network-forming position. Now it appears that, when the Mg^{2+} ion is present in a large concentration, it shows a tendency to occupy more and more the network-forming positions; such a network is poor in oxygen ions, so that the Mg^{2+} ion can compete successfully against the Si^{4+} ions. This effect is clearly demonstrated in *fig.* 13 (measurements taken at 1.5 × 10^6 c/s), which is most instructive when compared with fig. 4. Whereas in the latter diagram the dielectric losses show the previously discussed deep minimum at the intermediate concentrations of Na^+ and Li^+ ions, the curve in fig. 13 (where two Li^+ ions have been replaced by one Mg^{2+} ion) shows that with small Mg^{2+} concentrations in the glass the curve for the losses follows an analogous trend, but with higher Mg^{2+} concentrations makes a turn and ends at a very low level, such due to the fact that part of the Mg^{2+} ions no longer contribute towards the losses. As a result of the Mg^{2+} ions changing over from network-modifying to network-forming positions, the value of R, going to the right, drops (in fig. 4 R is constant), and this in itself already leads to a further reduction of the losses.

This picture of the situation is illustrated by *fig. 14,* for the case where two Li^+ ions are replaced by one Ni^{2+} ion. This curve resembles very much that of fig. 13, and in this case it is indeed possible to conclude from the change in colour of the glasses examined that, going to the right, more and more Ni^{2+} ions occupy the network-forming positions.

Finally, it is to be mentioned that, measured at $f = 10^{10}$ c/s, the replacement of two Li^+ ions by one Mg^{2+} ion yields a curve not showing any deflection but retaining the normal shape with a deep minimum. At these frequencies, where the vibration losses play a part, it is of no consequence whether the Mg^{2+} ion occupies a network-forming or a network-modifying position. By way of illustration reference is made to fig. 8.

Summary. The dielectric losses in glass arise from three causes: conduction, after-effect and resonance. The various forms of losses are described, it being shown that the conduction losses are of importance only at very low frequencies and high temperatures. The after-effect losses can be divided into "relaxation losses", occurring at room temperature in the frequency range of 10^{-3} to 10^6 c/s and shifting towards higher frequencies as the temperature rises, and "deformation losses", which are approximately proportional to the frequency and are particularly of importance at low temperatures. The resonance or vibration losses occur mainly at high frequencies (10^{10} to 10^{13} c/s) and as the temperature rises probably shift towards lower frequencies. The influence of the chemical composition and the structure of the glass upon the various losses is investigated, special attention being paid to the borate glasses, in which an accumulation region and a destruction region are to be distinguished according to the composition. It is indicated how the losses can be reduced in certain frequency ranges, some examples being given. Finally, it is shown how the dielectric losses can be taken as indications of the changes taking place in the structure of a glass when its composition is modified.

ABSTRACTS OF RECENT SCIENTIFIC PUBLICATIONS OF THE N.V. PHILIPS' GLOEILAMPENFABRIEKEN

Reprints of these papers not marked with an asterisk can be obtained free of charge upon application to the address on the back cover.

1981: P. C. van der Willigen: Grepen uit de ontwikkeling van het booglassen (Electro-techniek **29**, 143-147, 1951, No. 8). (Some remarks on the development of arc welding; in Dutch.)

Two important questions in the field of electric arc-welding by hand are discussed in this article. The first part deals with the choice between direct current and alternating current. Their advantages and disadvantages are described, including the question of the open circuit voltage of the welding transformer. In the second part the different methods for welding of steel are examined from the point of view of shielding of the deposited metal against nitrogen and oxygen from the air. In this connection the use of hydrogen and its influence on the weld are also briefly discussed.

1982: N. Warmoltz: On the application of a Philips ionization gauge type of ion source in a mass spectrometer leak detector (Appl. sci. Res. **B2**, 61-65, 1951, No. 1).

A system of electrodes as in the Philips ionization gauge can function as ion source giving a diverging ion beam in which the ions have different velocities. When placing this source behind a slit, it is possible to focus all the ions of the same mass in a second slit by combining a magnetic field parallel to the slits with an electric field perpendicular to the slits and to the line joining the slits. Between the slits the ions describe a kind of epicycloidal trajectories. In this way it is possible to construct a simple leak detector.

1983: C. J. Bouwkamp and H. Bremmer: A note on Kline's Bessel-function expansion (Proc. Kon. Ned. Akad. Wetensch. Amsterdam A **54**, 130-134, 1951, No. 2).

A certain combination of Bessel functions, viz. J_ν $(\nu \sec \vartheta)$ Y_ν $(z + \nu \sec \vartheta)$ $-$ Y_ν $(\nu \sec \vartheta) J_\nu$ $(z + \nu \sec \vartheta)$, in which ν, ϑ, z are complex numbers, is expanded in a power series in the variable $1/\nu$. This series converges if $|\nu| > |z \cos \vartheta|$. The first three coefficients are given explicitly.

1984: J. H. van Santen and G. H. Jonker: Combinaisons ferromagnétiques du manganèse à structure pérovskite (J. Phys. Radium **12**, 202-204, 1951, No. 3). (Ferromagnetic combinations of manganese with perovskite structure; in French.)

From investigations on the magnetic behaviour of ferromagnetic mixed crystals with perovskite structure of the type $(1-x)$ $\mathrm{LaMn^{III}O_3 \cdot x Me\,Mn^{IV}O_3}$ (Me = Ca, Sr or Ba) it seems probable that the (indirect) exchange interaction between $\mathrm{Mn^{IV}}$ and $\mathrm{Mn^{IV}}$ is negative and that between $\mathrm{Mn^{III}}$ and $\mathrm{Mn^{III}}$ is positive. This is the first known example of a positive indirect exchange interaction in oxidic compounds.

1985: J. J. Went: Linear magnetostriction of homogeneous nickel alloys (Physica **17**, 98-116, 1951, No. 2).

The magnetostriction of homogeneous Ni-alloys is investigated. The magnetostriction is measured as a function of the composition of the alloy, of the induction caused by an external magnetic field and of the temperature. A comprehensive table of data is given. Several general relationships for binary alloys have been found. The saturation magnetostriction λ_s at 0 °K can be predicted if the saturation induction I_s is known; λ_s at a higher temperature follows directly from the λ_s value at 0 °K and the relation I_s vs T (except for Ni-Mn-alloys). A single relationship has been found between λ and I for alloys except those containing Co or Mn. From all these data the magnetostriction for ternary alloys may be calculated.

1986: G. W. Rathenau and G. Baas: Grain growth in a texture, studied by means of electron-emission microscopy (Physica **17**, 117-128, 1951, No. 2).

Grain growth and secondary recrystallization in rolled face-entered Ni-Fe-alloys has been studied by electron-optical means, an image of the activated hot metal surface being formed. Grain growth in an imperfect cubic texture proved to be a discontinuous process. Almost all neighbouring grains invade quickly one grain or group of grains. Grain-boundary movement at low-energy boundaries occurs on a small scale. The high-energy parts of the boundary between a cubic crystal and its (near) twin proved to move in a direction parallel to the common (111) plane. The surface tension of the boundary between a secondary crystal and a cubic crystal which is to be absorbed is about twice the value corresponding to the surface between two cubic crystals.

R 160: H. Bremmer: The discharge of a series of equal condensers having arbitrary resistances connected in parallel (Philips Res. Rep. **6**, 81-85, 1951, No.2).

This paper concerns the discharge of a series of condensers through a ballistic galvanometer if a variable resistor is connected in parallel to each condenser, in connection with the model described in **R 159**. The flow of current through the galvanometer is calculated with the aid of the operational calculus.

R 161: B. D. H. Tellegen and E. Klauss: Resonant circuits coupled by a passive four-pole that may violate the reciprocity relation (Philips Res. Rep. **6**, 86-95, 1951, No. 2).

The system of two resonant circuits coupled by a passive four-pole that may violate the reciprocity relation is investigated. To obtain the maximum transfer for a given form of the resonance curve, the circuits must be equally damped and equally tuned. To obtain the maximum transfer with two circuits coupled by a passive four-pole satisfying the reciprocity relation, the circuits must generally be unequally damped and unequally tuned. When the coupled circuits are used as an interstage network in an amplifier, to minimize the influence of changes in valve capacitances on the shape of the resonance curve, the circuits should be equally damped and equally tuned. For symmetrical, flat-topped resonance curves the maximum transfer with non-reciprocal coupling four-poles, the ratios of the maximum transfer with reciprocal coupling four-poles to the transfer with reciprocal transfer with reciprocal coupling four-poles and to equally damped and equally tuned circuits are $(1 + \sqrt{2}) : 2 : 1$.

R 162: H. G. Beljers and W. J. van de Lindt: Dielectric measurements with two magic tees on shorted wave guides (Philips Res. Rep. **6**, 96-104, 1951, No. 2).

A description is given of the method and calculations underlying dielectric measurements at microwaves with the aid of wave guides. It is shown that a „magic Tee" (a certain arrangement of four branches of rectangular wave guides at one junction) can be used both as a bridge and as means of establishing any complex waveguide impedance. By using these Tees dielectric measurements can be carried out with greater accuracy than in the conventional method with a standing-wave detector. Some details of the construction of the apparatus and the measurement are given. In conclusion a dielectric measurement of polystyrene is dealt with.

R 163: H. C. Hamaker and Th. Hehenkamp: Minimum-cost transformers and chokes, II (Philips Res. Rep. **6**, 105-134, 1951, No. 2).

In the foregoing paper **R 150** the equations specifying a transformer design with minimum price, *P*, when the apparent power, VA, and the losses, *W*, are prescribed, were solved, and the chief characteristics of the resultant designs were discussed. This we shall call the P-W-class of designs. In the present paper two alternative classes of designs are considered, namely, (1) the P-M-class of designs giving minimum price for prescribed values of the power, VA, and the product, $M = BS$, of the peak magnetic flux density and effective electric-current density; and (2) the W-M-class of designs giving minimum losses, *W*, when VA and *M* are prescribed. The solutions obtained are casted in such a form that they are directly comparable *inter se* and with the P-W-solution of the foregoing paper. When power and losses are prescribed the P-W-class of designs is always cheapest, but if instead of the losses we prescribe a value of *B* or of the specific dissipation of heat, v, per cm^2 of external surface, the other classes of designs may be preferable. It is shown that the choice of a design depends mainly on the transformer characteristics which are considered as the limiting factors; a choice between the three classes of designs is of secondary importance. These problems are discussed in detail. In the appendix, a set of tables is provided by means of which the P-M-designs or the W-M-designs can be rapidly obtained. A concluding section deals with the problem of a design such that the sum of the cost of the transformers and the cost of the electric power dissipated as heat during its life, is at a minimum. This problem can also be solved by the methods developed.

R 164: P. Schagen: On the mechanism of high-velocity target stabilization and the mode of operation of television-camera tubes of the image-iconoscope type (Philips Res. Rep. **6**, 135-153, 1951, No. 2).

In this article the mechanism of the high-velocity target stabilization in the iconoscope and the image iconoscope is described. Some hypotheses are formulated for the mechanism of the image iconoscope, and equations are derived therefrom for the potential of target elements as a function of time and for the signal output of these tubes. This theoretical approach indicates that an increase in the secondary-emission coefficient of the target and in the target capacitance will result in better picture quality. Experiments confirm these predictions.